Theses and Dissertations

1-1-1980

On electronic measurement of fluidic velocity in electrolytes.

Wayne S. Groh

Follow this and additional works at: http://preserve.lehigh.edu/etd

Part of the Electrical and Computer Engineering Commons

Recommended Citation

ON ELECTRONIC MEASUREMENT OF

FLUIDIC VELOCITY IN ELECTROLYTES

by

Wayne S. Groh

A Thesis

Presented to the Graduate Committee

of Lehigh University

in Candidacy for the Degree of

Master of Science

in

Electrical Engineering
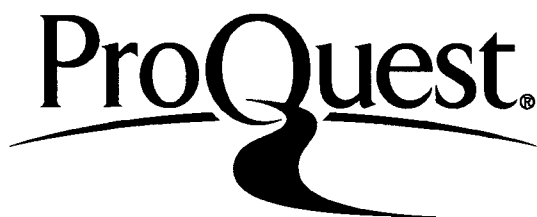
Lehigh University

1980

ProQuest Number: EP76578

![ProQuest logo]

ProQuest EP76578

This thesis is accepted and approved in partial fulfillment
of the requirements for the degree of Master of Science in
Electrical Engineering.

Dec. 12. 1980

(date)

_____
Professor in Charge

_____
Chairman of Department

-ii-

ACKNOWLEDGEMENTS

TABLE OF CONTENTS

LIST OF FIGURES

LIST OF TABLES

ABSTRACT

After a brief account of the mechanisms involved in electrolytic
conductance, several experiments are reported which are designed to
investigate the possibility of measuring velocity of an electrolyte
in an electrolytic cell by correlating it to changes in conductance.

The time dependent current is observed after turning the voltage
on or off. This is done at various cell voltages, electrolytic
velocities, concentrations and temperatures.

The effect of polarization is found to be dominant at low
voltages. At higher voltages the observed velocity dependence cannot
be explained by polarization changes alone.

It is found that too many variables are involved and that
absolute velocity measurements, therefore, would be difficult to base
on the observed behaviour of conductance. In special cases, however,
if for instance a zero velocity reference cell in the same electrolyte,
and at the same temperature, can be employed, it seems to be well
possible to measure velocity over a limited range.

INTRODUCTION

The purpose of this paper is to investigate whether flow
velocity of an electrolyte can be measured by making use of the fact
that often the conductance between electrodes is found to be depen-
dent upon the velocity of the electrolyte. Those effects are known
but do not seem to be clearly understood.

We have performed several measurements with thin platinum wire
electrodes in the stream of an electrolyte. In some cases we were
able to develop a qualitative understanding of the observed behav-
iour; in other cases the explanation remains purely hypothetical.
We believe, however, that our results nevertheless give some indica-
tion as to the usefulness and limitations of the approach.

1. REVIEW OF ELECTROLYTIC CONDUCTANCE THEORY

This chapter presents a general overview of electrolytic conductance theory. Emphasis is placed upon the theories of Faraday, Arrhenius and Debye and Hückel. The effects of concentration and temperature on strong and weak electrolytes are discussed. The broad topics of polarization and depolorization are addressed in order to obtain some understanding of the complex phenomena involved in electrochemical cells. To develop and enhance comprehension of the ideas presented, examples are given throughout the chapter including the electrolysis of a salt solution using platinum electrodes - identical to the setup used in our experimental efforts except for the fact that we used both resting as well as flowing solutions.

1.1 Electrolysis and Faraday's Laws of Electrolysis

Ohm's law may be applied to aqueous solutions as well as to metallic conductors, although application of the equation $V = IR$ is less obvious for electrolytes for several reasons: (a) current flow may heat the solution resulting in a strong decrease in electrolytic resistance, (b) the electrolysis due to current flow may cause the electrodes to become coated with the insulating films and (c) currents can induce depletion or accumulation of charges. Whereas metallic conduction is due to the movement of electrons through a conductor to which a potential is applied, electrolytic conduction is due to and depends upon the characteristics and the quantities of moving ions contained in the solution. Ion migration, as it is

called, is the transfer of charge between cell electrodes as well as the transport of matter from one part of the conductor to another. Electronic conductors experience an increase in resistance for an increase in temperature, while electrolytic conductors experience a decrease in resistance. Finally, when current flows in electrolytic conductors, chemical reactions occur at the electrodes.

A simple example will serve to illustrate the described phenomena of electrolytic conduction. Consider an electrolytic cell as shown below with inert platinum electrodes immersed in a solution of water and sodium chloride.
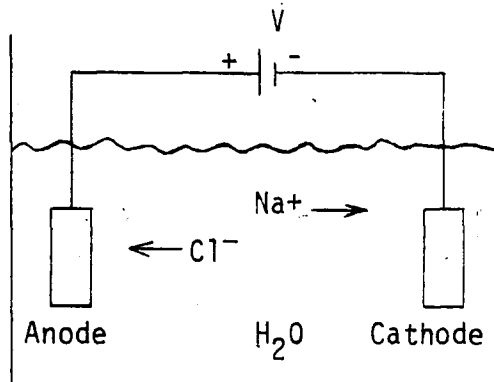
Fig. 1 - Simple electrochemical cell

Platinum is a desirable electrode material which greatly reduces the extent to which ions of an electrode will go into or out of solution. Sodium chloride consists of a crystal of ions which will completely dissociate into Na^+ and Cl^-. The solution is therefore a strong electrolyte. Applying the potential V, results in the following electrode reactions:

1) At the cathode:

$$Na^+ + e \rightarrow Na$$
$$Na + H_2O \rightarrow NaOH + H_2\uparrow$$
$$NaOH \rightarrow Na^+ + OH^-$$

2) At the anode:

$$2Cl^- - 2e \rightarrow 2Cl$$
$$2Cl + H_2O \rightarrow 2HCl + O_2\uparrow$$
$$HCl \rightarrow H^+ + Cl^-$$

or

$$2Cl^- - 2e \rightarrow 2Cl$$
$$Cl + H_2O \rightarrow HCl + OH$$
$$OH + OH \rightarrow H_2O_2$$
$$2H_2O_2 \rightarrow 2H_2O + O_2\uparrow$$

or

$$2Cl^- - 2e \rightarrow 2Cl$$
$$2Cl + 2Cl \rightarrow 2Cl_2\uparrow$$
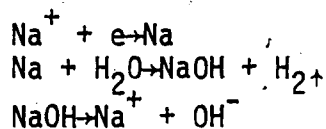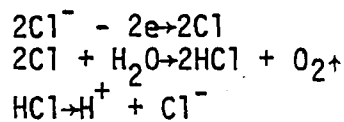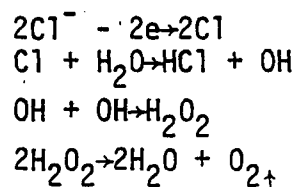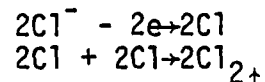
The last two reactions would take place if there were not a plentiful supply of H_2O in the vicinity of the anode as there is for the occurrence of the middle set of anode reactions. In the experiments we performed, the flow of a salt solution over platinum electrodes should eliminate the possibility of the last two reactions occurring at the anode. Due to the applied potential, anions migrate to the anode and cations to the cathode. Movement of charged species results in a current with each ion carrying a portion of it. Current passing through an electrolytic conductor with electrons entering and leaving the solution due to chemical changes at the electrodes in addition to ion migration through the solution is called electrolysis. Faraday's laws of electrolysis explain the fact that equal numbers of electrons enter and leave the solution, as will now be discussed.

-5-

About 1833, Faraday found that the reaction at the anode may be
any oxidation reaction (species losing electrons) that is feasible
and that the reaction at the cathode may be any one of a reduction
(species gaining electrons). His first law of electrolysis states:
The amounts of primary products involved in reaction at the elec-
trodes during electrolysis is directly proportional to the amount of
electricity passed through the solution. Considering the electrol-
ysis of copper sulphate using copper electrodes will illustrate this
law. Copper sulphate ionizes as

$$CuSO_4 \rightarrow Cu^{++} + SO_4^{=}$$
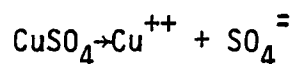
in solution, and during electrolysis the copper cation and the sul-
phate anion migrate to the cathode and anode respectively. At the
cathode, the cation is discharged by the electrons present in the
cathode resulting in the deposition of copper atoms:

$$Cu^{++} + 2e^- \rightarrow Cu$$
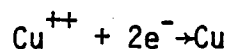
To maintain a supply of electrons at the cathode, copper atoms from
the anode are ionized by the reverse process occurring at the
cathode, i.e.,

$$Cu \rightarrow Cu^{++} + 2e^-$$
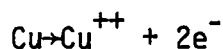
Assuming the solution is not stirred and that the rates of electrode
processes are adequately large, copper ions may tend to build up in
the vicinity of the anode while a depletion of the same may occur
near the cathode. The migration of sulphate anions towards the
anode, however, maintains the required electrical balance. Hence the
overall reaction in the cell is the transference of copper atoms from
the anode to the cathode: $Cu_a \rightarrow Cu_c$. Now consider the movement of the

charges. At the anode, for one copper atom that is ionized, two
electronic charges are released and at the cathode, two electronic
charges are required for one copper atom to be discharged. In other
words, the dissolution of a unit amount of copper and the deposition
of the same amount is associated with the same, constant amount of
transferred charge.

Faraday's second law of electrolysis states that the flow of a
given amount of electricity causes the primary products to be formed
in the ratio of their equivalent weights. Another example will prove
useful. Consider the general reaction at the cathode of a metal ion,
M^{z+}, of valency z, discharging,

$$M^{z+} + ze^- \rightarrow M$$
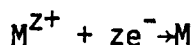
where each ion of the metal carries z electronic charges. Since one
gram atom (mole) of a metal contains Avogadro's number of atoms, N,
there are N/z atoms in one gram equivalent. Each atom yields one ion
so that one gram ion of the metal contains N/z ions. Since one gram
ion of metal carries N charges, both of which (N and the charge) are
constants, then one gram ion of a metal carries a constant amount of
electricity. This amount is known as one Faraday, F, and is equal
to the product of N and e where $N = 6.023 \times 10^{23}$ and $e = 4.803 \times 10^{-10}$ absolute electrostatic units $= 1.602 \times 10^{-19}$ absolute coulombs:
$F \approx 96,500$ coulombs/gram equivalent. During electrolysis, one Faraday
liberates one gram equivalent of a metal from its ions. In other
words, the passage of one Faraday of electricity removes Avogadro's
number of electrons from the cathode by reducing one equivalent of·

material and donates the same number to the anode due to oxidation of some material.

1.2 Electrolytic Conductance

Ohm's law may be used to determine the resistance of an electrolytic solution but instead of resistance, its reciprocal, conductance, is usually the quantity under observation and of discussion. Consider two parallel, metal plates of cross-sectional area A and of resistivity ρ (ohm-cm) separated by a distance L. When immersed in a solution the resistance between the plates is

$$R = \rho \frac{L}{A}$$

Defining the reciprocal of resistivity as conductivity, K, with units of mhos/cm it follows that K = L/AR. Equivalent conductance is defined as one thousand times the conductivity divided by the concentration expressed in equivalents of solute per liter of solution, [1], i.e.,

$$\Lambda = \frac{1000K}{C}$$

and has units of mhos/equivalent. It is noted that conductivity is a function of concentration and that the equivalent conductance of electrolytes varies with temperature and concentration. For constant temperatures, as concentration decreases Λ increases and in some cases (usually strong electrolytes) extrapolation of Λ to zero concentration yields a finite value, Λ_0:

$$\Lambda_0 = \lim_{c \to 0} \Lambda$$

-8-

Fig. 2 depicts the Λ and C relationship and Fig. 3 shows that by plotting $\sqrt{C}$ along the abscissa, as proposed by Kohlrausch, finding Λ_0 by extrapolation is made easier. From the plot of Λ vs. $\sqrt{C}$ it is obvious that extrapolation to zero concentration is futile for the two lowest curves - those of weak electrolytes. For approximate calculations, and over appropriate ranges, Λ may be assumed constant as concentration changes. Therefore, if Λ, L and A are constants it follows from K = L/AR and Λ = 1000K/C that R = constant/C. Now using Ohm's law with a constant applied voltage one finds that the current is directly proportional to the concentration. This is a useful approximation except when Λ cannot be considered independent of concentration - which occurs for concentrations greater than about one normal.

The conductance of all electrolytes is noted to increase as temperature increases. The limiting equivalent conductance depends upon temperature as follows: [2]

$$\Lambda_{o(t)} = \Lambda_{o(25°C)}[1+\beta(t-25)]$$

where $\Lambda_{o(t)}$ is the limiting equivalent conductance at temperature t°C and $\Lambda_{o(25°C)}$ at 25°C. β is a constant, which for salts, is in the range 0.022 to 0.025, therefore, Λ_0 increases by 2.2% to 2.5% per degree centigrade.

Arrhenius theorized that decreasing concentrations lead to increasing equivalent conductances due to a greater degree of dissociation of electrolyte into ions. It follows that at zero concentra-
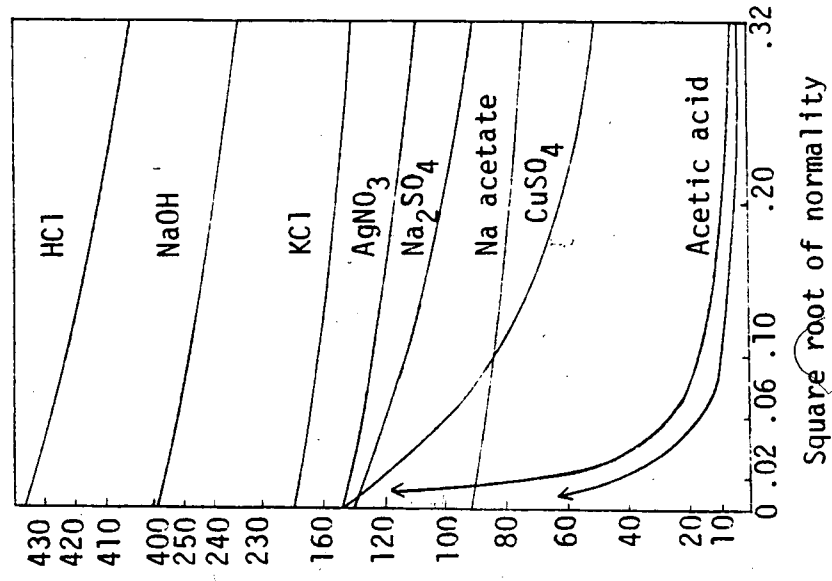
Fig. 3 - Kohlrausch square-root law for equiva-
lent conductance of aqueous electro-
lytes at 25°C (Potter [6], p. 23)

HCl

NaOH

KCl

AgNO$_3$
Na$_2$SO$_4$
Na acetate

CuSO$_4$

Acetic acid

Square root of normality

.02 .06 .10   .20   .32

430
420
410
400
250
240
230

160

120

100

80

60

40

20
10

0
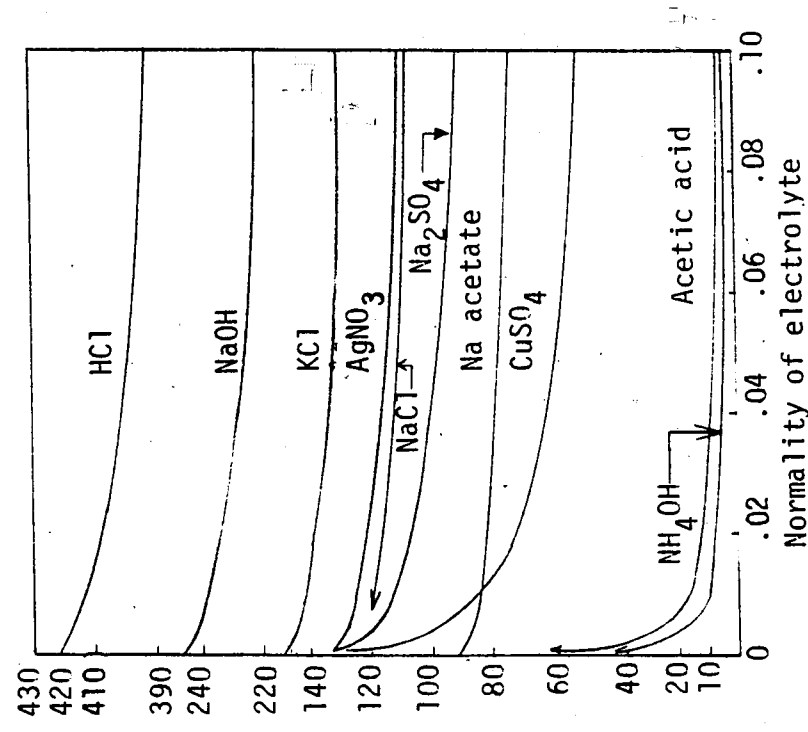
Fig. 2 - Concentration dependence of equiva-
lent conductance for aqueous solu-
tions at 25°C (Potter [6], p. 22)

HCl

NaOH

KCl
AgNO$_3$
NaCl
Na$_2$SO$_4$
Na acetate

CuSO$_4$

NH$_4$OH
Acetic acid

Normality of electrolyte

0   .02   .04   .06   .08   .10

430
420
410

390
240

220

140

120

100

80

60

40

20
10

0

tion, dissociation would be complete and Λ reaches a maximum value, Λ_0, such that at some non-zero concentration, C, the degree of dissociation corresponds to Λ/Λ_0. This theory appears reasonable for weak electrolytes, but not for strong electrolytes because they are already completely dissociated into ions due to their ionic crystalline structure. Hence discussion of the dissociation of strong electrolytes is not appropriate, although the extent of ionic interaction is. Here the theory of Debye and Hückel must be considered.

At this point, both theories will be reviewed.

1.2.1 Arrhenius Theory of Partial Dissociation

In 1887 Arrhenius proposed that electrolytic solutions contain positive and negative ions and that the entire solution is neutral since positive and negative charge densities are equal.

Arrhenius also suggested that an electrolytic solution may consist of ions as well as neutral molecules of the substance in an equilibrium. Therefore, the degree of dissociation will increase, as the concentration of dissolved substances decreases. This view implies that only infinitely dilute solutions (concentration tending toward zero) will exhibit complete dissociation, and that solutions of finite concentrations will have a partially ionized electrolyte - the degree of ionization depending upon the particular substance and its concentration.

Since the colligative properties (vapor pressure lowering,

-11-

boiling point elevation, freezing point lowering and osomtic pressure)
of a dilute solution are solely a function of the number of particles
in the solvent, Arrhenius' theory of partial electrolytic dissociation
could be used to explain these properties. In other words, a solution
with ions versus one without ions will contain more particles. Assum-
ing that colligative properties are affected equally by ions and
neutral molecules, the increased number of particles in solution
should yield an increase in the colligative effects. For example a
nonelectrolyte in water has a molal freezing point constant of 1.86°C
per mole per 1000 gm of solvent. Assuming dilute solutions and hence
complete dissociation, an electrolyte which yields three ions per
molecule of substance should have a molal freezing point constant
triple that of the nonelectrolyte. Specifically potassium sulphate
yields three ions upon complete dissociation resulting in a molal
freezing point constant of 3 x 1.86°C = 5.58°C. The four ions of
completely dissociated potassium ferricyanide yield 4 x 1.86°C =
7.44°C as its molal freezing point constant. It is noted that these
values are limiting ones since complete dissociation was assumed,
i.e., a dilute solution. Tables of observed data of $\Delta T_f/m$ (the ratio
of the freezing point lowering to the molality) for various concentra-
tions reveal that the limiting molal freezing point constants are in
agreement with Arrhenius' theory of partial electrolytic dissociation
(see Table I)

Since Arrhenius' theory of partial electrolytic dissociation
accounts for molal freezing point constants greater than 1.86°C
and lower than the limits due to complete dissociation, it is

-12-

Table I

$\Delta T_f/m$ For Aqueous Solutions Of Electrolytes[1]

m	HCl	HNO_3	NH_4Cl	$CuSO_4$	H_2SO_4	$CoCl_2$	K_2SO_4	$K_3Fe(CN)_6$
0.0005	-	-	-	-	-	-	-	7.3
0.001	3.690	-	-	-	-	-	5.280	7.10
0.002	3.669	-	-	-	-	5.35	-	6.87
0.0025	-	-	-	3.003	5.052	-	5.258	-
0.005	3.635	3.67	3.617	2.871	4.814	5.208	5.150	6.53
0.01	3.601	3.64	3.582	2.703	4.584	5.107	5.010	6.26
0.05	3.532	3.55	3.489	2.266	4.112	4.918	4.559	5.60
0.10	3.523	3.51	3.442	2.08	3.940	4.882	4.319	5.30
0.20	3.54	3.47	3.392	1.91	3.790	4.946	4.044	5.0
0.40	-	3.46	-	-	3.68	5.170	3.79	-
1.00	3.94	3.58	3.33	1.72	4.04	6.31	-	-
2.00	4.43	3.79	3.34	-	5.07	8.51	-	-
4.00	5.65	4.16	3.35	-	7.05	-	-	-

possible to calculate the degree of ionization of an electrolyte using observed colligate data or using the values of "i" which are calculated from the colligative data. The result is [3]

$$\alpha = \frac{i-1}{\nu-1}$$

which may be applied to any colligative property, where α is the degree of dissociation of an electrolyte $A_x B_y$. The number of ions of A is x and that of B is y. Therefore one molecule of electrolyte yields $\nu = x + y$ ions. The parameter "i" is the van't Hoff factor and relates how much greater the colligative effect of an electrolyte is than the effect of a nonelectrolyte of equal concentration. For example, if ΔT_f is the freezing point lowering for an electrolyte and $(\Delta T_f)_0$ for a nonelectrolyte, then the van't Hoff factor becomes

$$i = \frac{\Delta T_f}{(\Delta T_f)_0}$$

Arrhenius' theory of partial electrolytic dissociation

---

[1]Prutton [2], p. 211.

-13-

satisfactorily accounts for the colligative behaviour, electrical conductance, and ionic equilibria of weak electrolytes in dilute solutions.

1.2.2 Debye-Hückel Theory of Interionic Attraction

In 1923, P. Debye and E. Hückel simplified the mathematically rigorous treatment of interionic attraction in strong electrolytes by S. R. Milner. They assumed that ions exist in solutions of strong electrolytes, but, unlike Arrhenius, they did not assume that partial dissociation was the cause of the unconformable properties of strong electrolytes. Instead, they conceived of complete ionization, at least for dilute solutions, with the effects being due to interionic attractions creating unequal distributions of ions. With a mathematical argument and application of Coulomb forces between ions (see Résibois, Electrolyte Theory, p. 28), Debye and Hückel showed that "each ion in solution is surrounded by an ionic atmosphere whose net charge is opposite to that of the central ion". [4] Characteristics of the electrolyte are affected by the interaction between the central ion and its atmosphere. The atmosphere is a function of the number of ions in solution, their valencies, the temperature, and the dielectric constant of the medium. For a constant temperature and a given medium the electrolyte should exhibit properties depending only upon ion charges and ion concentration. Due to the mathematical simplifications made by Debye and Hückel, the above conclusions are valid only for very dilute solutions.

Discussion of the reasons for the higher accuracy of the Debye-Hückel theory as compared to Arrhenius' theory in explaining the behaviour of strong electrolytes in dilute solutions is complex and lengthy. Instead Fig. 4 (from Bjerrum) will serve as an illustration. A measure of interionic attractions is (1-g), where g,
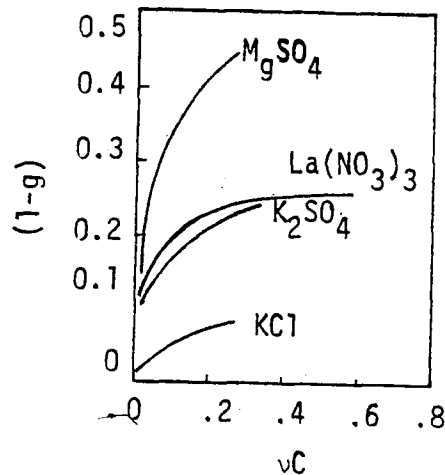
Fig. 4 - Plot of (1-g) vs. νC for strong electrolytes (Prutton, [2], p. 219)

the osmotic coefficient, is defined as i/ν; i is van't Hoff's factor and ν is the total number of ions from one molecule of the electrolyte. Therefore the abscissa in Fig. 4, νC, represents the concentration of ions in solution. Another way of envisioning the meaning of the ordinate, (1-g), is that it represents the deviation of observed effects for a solution of finite concentration from that of an infinitely dilute solution.

-15-

The Debye-Hückel theory predicts (for derivation see: Debye and Hückel, Physikalische Zeitschrift, 24, 185 (1923)) the following for strong electrolytes in water in dilute solutions at 0°C:

$$1-g = 0.264(z_+z_-)^{3/2} \sqrt{\nu C}$$

where z_+ is the valence of the cation and z_- the valence of the anion. This equation is of the form $y = mx$, therefore $(1-g)$ should have slopes depending upon the valence type when plotted against $\sqrt{\nu C}$. Fig. 5 shows verification of the equations from the theory. The
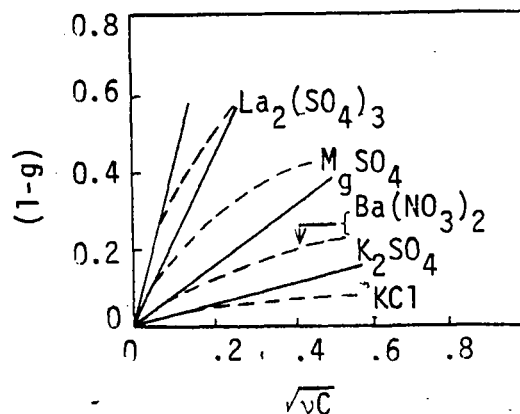
Fig. 5 - Plot of (1-g) vs. $\sqrt{\nu C}$ for various electrolytes

solid lines are the theoretical plots and the dotted lines are the experimental plots. [5] The plots show that the curves follow the valence type which the theory predicts - the larger the product of

-16-

z_+z_-, the larger the slope of the plot. In addition the plots show that the experimental data, for low concentration, approach the curves that are predicted by theory. It is inappropriate to compare the curves for concentrations greater than dilute because the Debye-Hückel theory included mathematical assumptions which were valid only for dilute solutions. In view of the discussion of complete ionization of strong electrolytes (see also Fig. 4) the above two observations of Fig. 5 reinforces the idea of interatomic attractions as being a reasonable explanation of the deviation in strong electrolytes. It is noted that in the limit of zero ionic concentration, complete dissociation occurs, resulting in no interionic attractions, hence $g = 1$ and $1-g = 0$ which is born out in the above equations.

The material presented heretofore discussed some of the basic concepts of electrolytic conductance theory. Attention now turns to the fundamental topics of polarization and depolarization which are more germane to the task of understanding the reactions which occur at the electrodes' surfaces. This understanding is important in regard to a velocity measurement.

1.3 Polarization

Polarization during electrolysis can be of two types - concentration polarization and/or overvoltage polarization. The former is due to concentration changes of an electrolyte around the electrodes resulting in an emf that opposes the applied voltage. The latter originates from irreverisble electrode processes and is therefore

-17-

dependent upon the type of electrode as well as the surface reactions at the electrode.

1.3.1 Concentration Polarization

In order for electrolysis to be continuous at the electrodes there must be a continuous supply of ions that are ready to be discharged. There are three ways how ions can get to the electrodes: (1) ionic migration, (2) ionic diffusion, and (3) mixing of the bulk region mechanically or by convection. A net diffusion of ions will not occur if the supply of ions due to migration and mixing is sufficient since the entire solution would then be essentially uniform. On the other hand, if ions are discharged at an electrode at a rate greater than they are brought to it - by migration and mixing - then the concentration of ions at the surface of the electrode decreases to a value below that of the bulk, and diffusion may occur. In all these cases a net positive or negative charge density may be present near an electrode thus changing (reducing) the electric field strength in the bulk region.

By increasing the applied voltage the rate of electrolysis may be increased resulting in the largest possible concentration gradient in the vicinity of the electrodes and hence nearly a zero ionic concentration at the electrodes. The current cannot increase much further; however, the electrode potential can increase because it is related to ionic concentration. [6] Corresponding to the greatest rate of the particular electrode reaction there exists,

therefore, a limiting value of current. The limiting value of current does not remain the same as the electrode potential (also called concentration polarization or concentration overpotential) increases beyond some value; another electrode reaction which has a larger limiting current would then occur, i.e., another type of ion would begin to discharge. Below is a graph (Fig. 6) illustrating this current vs. concentration overpotential relationship.
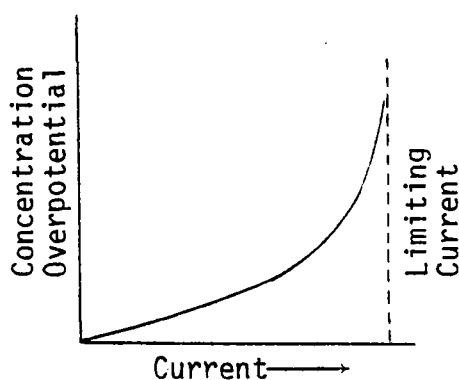
Fig. 6 - Variation of concentration overpotential
with current [6]

A specific example explaining the origin of concentration polarization is now given. Consider that a solution of silver nitrate is to be electrolyzed using silver electrodes. There is no initial back emf since the electrodes are the same and the concentration of silver nitrate is uniform in the solution. When currect flows, however, silver atoms from the anode dissolve into solution to

-19-

form silver ions ($Ag_{(s)} - e^- \rightarrow Ag^+$) and silver ions in the solution deposit on the cathode ($Ag^+ + e^- \rightarrow Ag_{(s)}$). The concentration of silver ions near the anode is greater than that in the bulk region of the solution and which in turn is greater than that near the cathode as seen by Fig. 7 where time is depicted as increasing vertically downward. As time progresses, the silver ions migrate toward the cathode due to the applied voltage and as seen in the figure, at each electrode, a polarization voltage develops which tends to send current, I_{pol}, in the opposite direction to the current that is due to the applied voltage.[1] It is worthwhile to consider the silver ion denoted by the broken arrow. The migration of this ion to the cathode is inhibited due to a shielding effect caused by the already present silver ions. Therefore, for a given current, the applied voltage must be increased to overcome this shielding effect.

Consider also the electrolysis of a sodium chloride solution using platinum electrodes as shown in Fig. 8 where ion clouds of Cl^- and Na^+ form at the anode and cathode respectively. It is important to note that both examples have the same direction of applied voltage, but in the first example there exists a buildup of positive charges at the anode and a depletion of positive charges at the cathode, while the second example exhibits a _sign_ reversal of the charges at the respective electrodes (note that with respect to

---

[1]Polarization voltage may formally be defined as voltage that opposes the applied voltage. It is caused by an emf due either to a chemical reaction (chemical cell) or to a concentration difference caused by a transfer of material (concentration cell), or both.

V applied

Ag | Silver nitrate soln | Ag

$+$ — — —

↓ time

Mean

$Ag_{(s)} - e^- \rightarrow Ag^+$ | Hi conc of Ag^+ | conc of Ag^+ in bulk | Low conc of Ag^+ | $Ag^+ + e^- \rightarrow Ag_{(s)}$

Silver is deposited on cathode

⊕
⊕⊕   ⊕ ⊕   ⊕⊕
⊕⊕⊕   ⊕ ⊕

Migration due to $V_{applied}$

⊕   ⊕   ⊕
⊕ ⊕   ⊕   ⊕⊕
⊕ ⊕ ⊕   ⊕

$Ag_{(s)} - e^- \rightarrow Ag^+$ | | | | $Ag^+ + e^- \rightarrow Ag_{(s)}$

Ag^+

⊕ ⊕   ⊕   ⊕
⊕ ⊕   ⊕   ⊕ ⊕
⊕ ⊕ ⊕

V_{pol} V_{pol}

I_{pol} I_{pol}
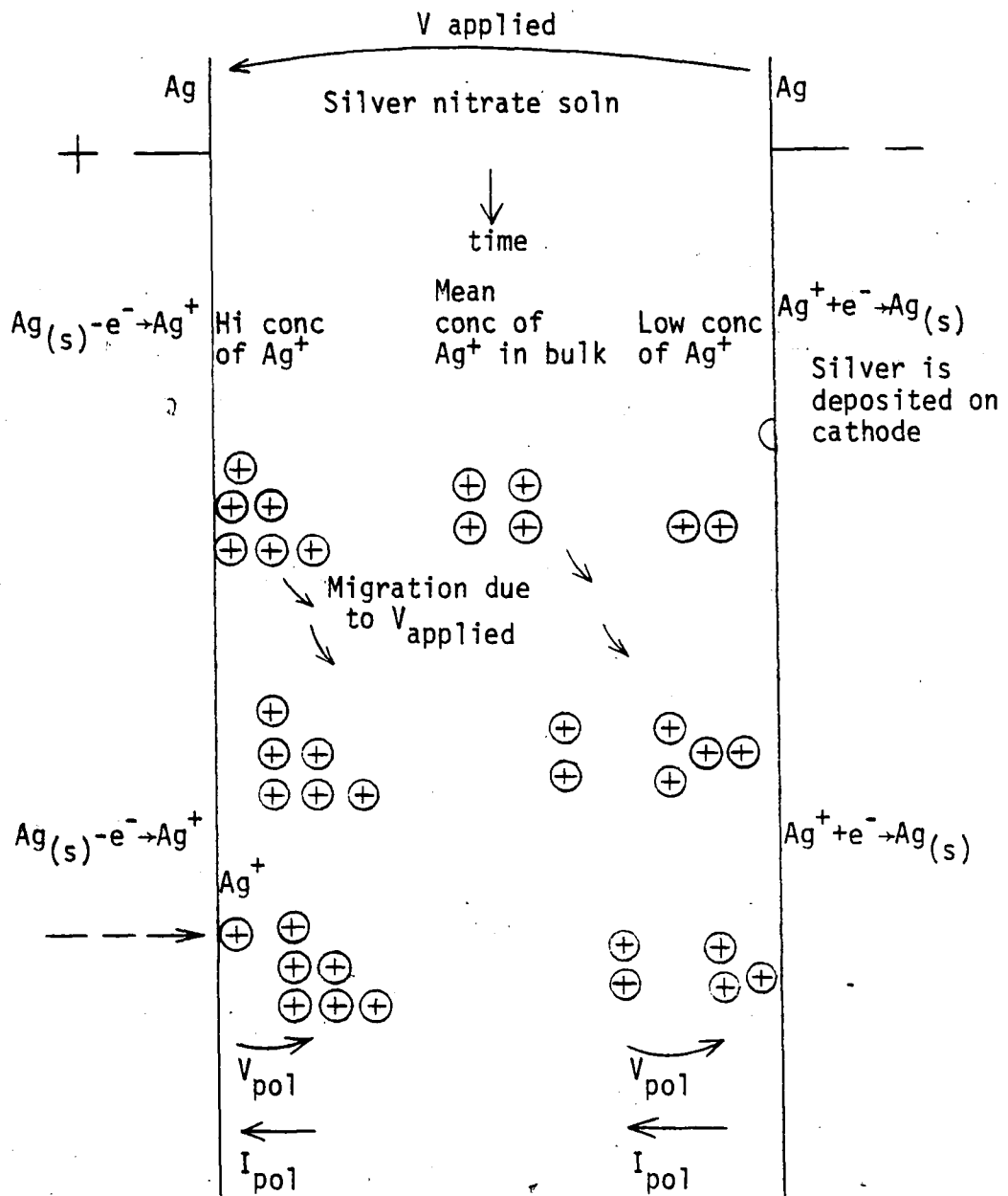
Fig. 7 - Development of concentration polarization

$$V_{applied}$$

$$+ \quad \longrightarrow \quad \vec{E}_{applied} \quad \longrightarrow$$

$$2Cl^- - 2e^- \rightarrow 2Cl$$
$$4Cl + 2H_2O \rightarrow 4HCl + O_2$$
$$HCl \rightarrow H^+ + Cl^-$$

$$Na^+ + e \rightarrow Na$$
$$2Na + 2H_2O \rightarrow 2NaOH + H_2$$
$$NaOH \rightarrow Na^+ + OH^-$$

$$Cl^- \qquad Na^+$$

$$V_{pol}$$

$$\vec{E}_{pol}$$
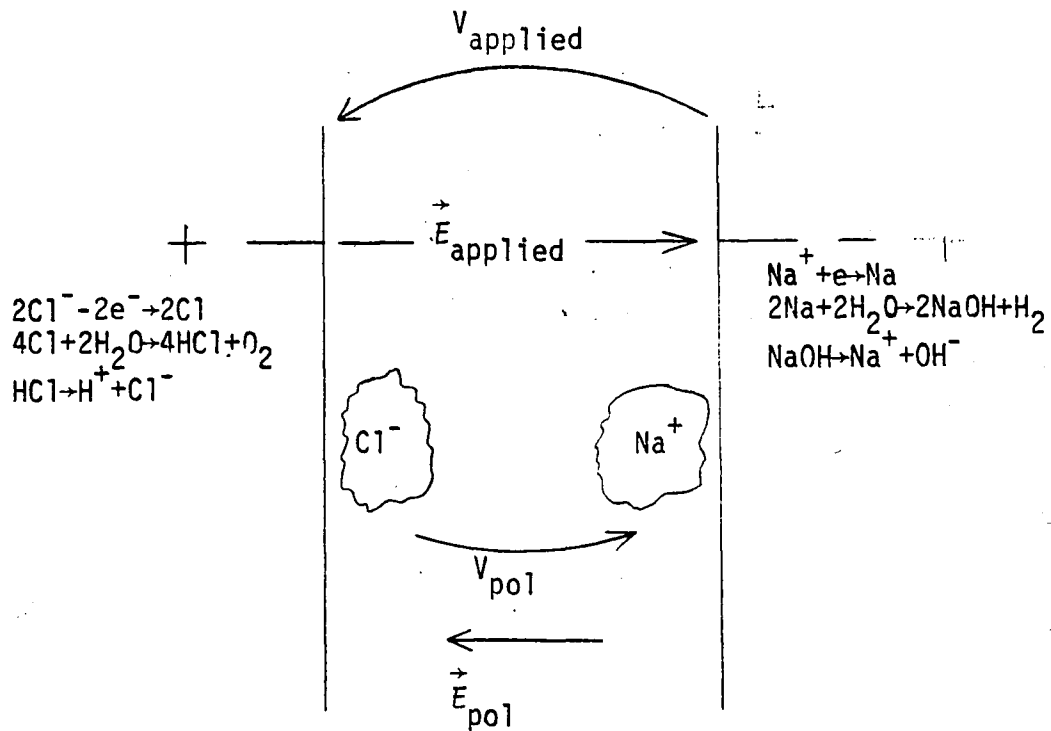
Fig. 8 - Example of concentration
polarization

sign, the opposite of a depletion of positive charges is a depletion of negative charges which in turn is electrically equivalent to an excess of positive charges). Nevertheless, in each example there exists a polarization effect which works to oppose the applied voltage.

1.3.2 Overvoltage Polarization

The second type of polarization, overvoltage polarization, is a resistance to charge transfer at an electrode and can arise from products of electrolysis as well as from IR drops across coatings on

electrodes or from both. The former is illustrated by the electro-
lysis of a copper sulphate solution using silver electrodes as shown
below in Fig. 9.
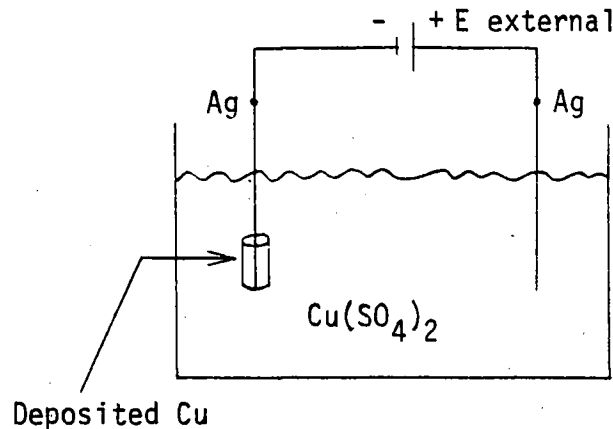
Fig. 9 - Electrolysis of a copper
sulphate solution

The voltage applied to the cell is

$$E_{\substack{applied \\ to\ cell}} = E_{external} - IR$$

where IR can be considered to be the voltage drop across the bulk of
the solution. The electrode reactions are given below with their
corresponsing standard electrode potentials at 25°C.

Cathode reaction ($\substack{deposition \\ of\ Cu}$)	$Cu^{++} + 2e^- \rightleftarrows Cu$	+ 0.337 volts
Anode reaction ($\substack{dissolution \\ of\ Ag}$)	$2Ag \rightleftarrows 2Ag^+ + 2e^-$	- 0.799 volts
Overall reaction	$Cu^{++} + 2Ag \rightleftarrows Cu + 2Ag^{++}$	- 0.462 volts = $E°$
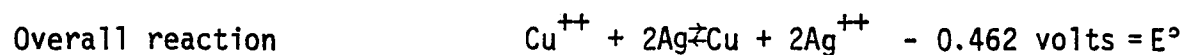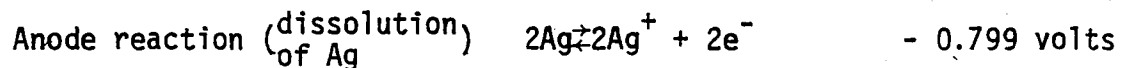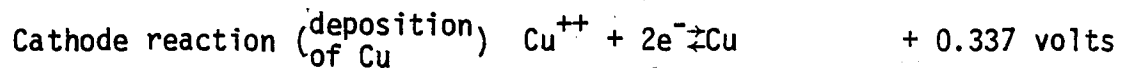
where $E°$ is the standard redox potential.

-23-

The concentration of Cu^{++} near the cathode decreases due to the deposition of copper on that electrode and correspondingly the concentration of Ag^+ near the anode increases due to silver going into solution. Since the ion concentration in the vicinity of each electrode is changing, then for a given amount of current the applied voltage must also change as seen from the Nernst equation (using activities, not concentrations, i.e., the activity coefficients do not equal unity).

$$E_{\substack{applied \\ to\ cell}} = E° - \frac{0.059}{n} \ln \frac{(a_{Ag^+})^2 (a_{Cu})}{(a_{Cu^{++}})(a_{Ag})^2}$$

$$= -0.462_v - \frac{0.059}{n} \ln \frac{(a_{Ag^+})^2}{(a_{Cu^{++}})}$$

where the activities of pure solids are set equal to one for reactions at moderate pressures, i.e., the metals are assumed to be in standard states; the solute exists at unit molality and one atmosphoric pressure, and n is the number of electrons/equivalent of product or the number of moles of electrons/mole of product. Hence there is a resistance to charge transfer because the negative sign of $E°$ means that the overall reaction is not spontaneous (as it would be for $E°$ greater than zero) and that energy must be put into the system - by increasing the external voltage - in order to carry out the reaction as written. Also, as time progresses the numerator and /denominator of the logarithm term will increase and decrease respectively. $E_{applied}$ will increase to a larger negative value and thus the external voltage required for sustained electrolysis will increase with time.   -24-

Overvoltage due to IR drops across electrode coatings is illustrated by the electrolysis of an acid solution using chromium electrodes as shown in Fig. 10. At the cathode chromium may go into solution, $Cr \rightarrow Cr^{+++} + 3e^-$, and the chromium ion reacts to form an
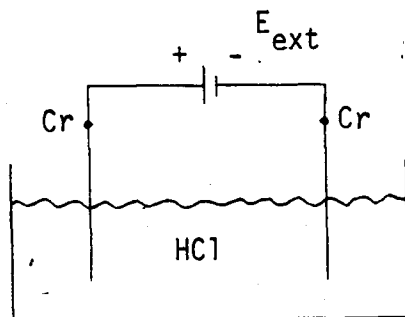
Fig. 10 - Electrolyzing an acid solution to form an oxide layer on the cathode

oxide layer on the electrode, $2Cr^{+++} + 3H_2O \rightarrow Cr_2O_3 + 6H^+$. The oxide layer inhibits charge transfer and presents an IR drop as denoted by a resistor (Fig. 11).
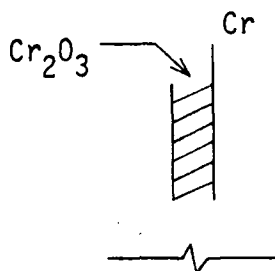
Fig. 11 - Oxidized chromium cathode; resistor symbolizing the electrical characteristics of the oxide layer

In the first example there is negligible IR drop across the deposited copper because copper is a good conductor. Therefore, each example separately describes each of the two means of contribution to over-

voltage polarization: products of electrolysis and electrode coatings which yield IR drops.

In the experiments that we performed, both zero and non-zero electrolyte velocities, and platinum electrodes were used. Therefore, concentration polarization was reduced as the velocity increased (equivalent to faster stirring) and any further observed polarization was most probably overvoltage polarization since "even the noblest metals, e.g., platinum, appear to form layers of oxide one or two molecules thick when oxygen is evolved on their surfaces." [7]

1.4 Depolarization

Depolarization results in a reduction of the effects caused by polarization. These effects, such as reduced cell current and increased electrode overpotential, generally result from an opposition to the cell's applied voltage. Depolarization can manifest itself in macroscopic as well as microscopic ways as shown by examples to follow. Species in solution which can be oxidized or reduced in addition to preventing oxygen or hydrogen evolution are called depolarizers. This can occur if the potentials needed for oxidation and reduction are lower than those for evolution of oxygen and hydrogen since the reactions requiring the lowest potentials are the ones which will occur. For cells consisting of inert electrodes, electrolysis of solutions which can produce only oxygen and hydro-

-26-

gen will result in the evolution of oxygen at the anode and hydrogen at the cathode. Although electrodes made of active metals allow either evolution of oxygen or dissolution of metal - depending upon the associated potentials, most of these active metals dissolve into solution because the oxygen overvoltage on them is large.

To illustrate depolarization on a macroscopic level, recall the discussion of polarization and Fig. 8 depicting the electrolysis of a sodium chloride solution with platinum electrodes. As time increases the polarization or shielding effect of the ion clouds becomes greater and current flow is therefore reduced. For a given applied voltage, increasing the velocity of the solution which flows over the electrodes tends to remove or wash away the ion clouds. Polarization is therefore reduced which results in an increased current flow - this effect, due to forces external to the chemical reactions of the cell, is a form of depolarization.

An example of electrode polarization and depolarization is now given to illustrate a form of depolarization which has both its origin and workings on the cell (microscopic) level, unlike the previous example which had an external origin for its depolarization. The evolution of hydrogen at a cathode involves several steps beginning with the combination of migration, diffusion and convection of hydrated hydrogen ions in the bulk region to the local area of the electrode. Upon arrival at the cathode the ions are discharged and dehydrated. Since a buildup of free hydrogen atoms cannot be main-

tained at the surface, [8] strong attachments of these free atoms to the electrode's surface (through valence bonds) is the accepted explanation of hydrogen discharging. This strong attachment is called adsorption [9] and results in the polarization of the electrode. Pairs of adsorbed hydrogen atoms combine to form hydrogen molecules which then undergo desorption from the metal surface into the solution. H_2 molecules are transported away from the electrode either by diffusing into solution or by combining to form bubbles (gas evolution) in the last step of hydrogen evolution. The above stages are outlined below and are taken from Potter, page 132.

1. $(H_3O^+)_B$ $\xrightarrow[\text{Convection}]{\text{Migration, Diffusion,}}$ $(H_3O^+)_E$

    Hydrated ion   Hydrated ion
    in bulk of solution   near electrode

2. $(H_3O+)_E + e$ $\xrightarrow[\text{Dehydration}]{\text{Discharge}}$ $M-H + H_2O$

    Ion   Electron   H atom adsorbed
       from metal M   on M

3. $M-H + M-H$ $\xrightarrow{\text{Combination}}$ H_2
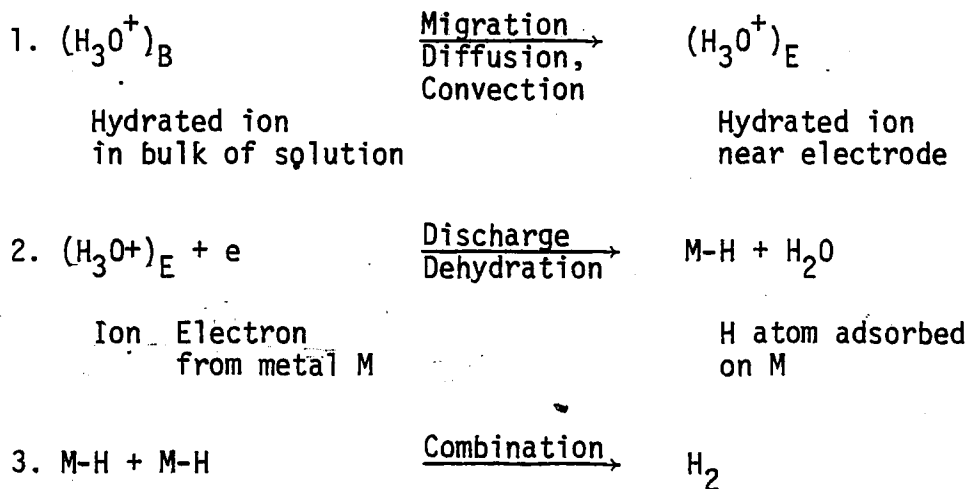
2. DESCRIPTION OF EXPERIMENTAL SETUP AND DATA ACQUISITION

The experimental setup has mechanical and electrical aspects.
An overall picture of the former is shown in Fig. 12. The electro-
lyte circulates through a continuous loop of 2500 ml capacity. The
plexiglass tower, T, collects the electrolyte in a resevoir, R,
above a vertical channel with a crossection of 0.59 cm x 8.35 cm and
a height of 25.05 cm. One wall, S, of the channel is removable by
sliding it out vertically. Attached to this wall are four horizontal
platinum wire electrodes, E, of 5 mils diameter. They are positioned
approximately in the center of the 0.59 cm channel. The probes were
about 2 cm in length. The uppermost probe is separated from the
second probe by 0.62 cm. The second and third probes are separated
by 1.30 cm. The spacing between the third and fourth probes is
0.62 cm. Fig. 13 shows the pertinent dimensions of the tower and
sliding panel. Referring to Fig. 12, the tower is connected to pump,
P. The flow rate of the electrolyte is controlled by use of values
V1 and V2. Rotameter, M, once calibrated by external means, was used
for velocity measurements of the electrolyte in the channel; flow in
the channel was laminar for most of the velocity range (see appendix
A1). From the top of the rotameter, plastic tubing is immersed in a
thermostatically controlled bath, B, which determines the electro-
lyte's temperature to about ±1°C. This tubing empties the electro-
lyte back into the resevoir. The rotameter was calibrated in the
following way: At several rotameter values, the time for a measured
volume of water to be pumped into a container was recorded. The ratio
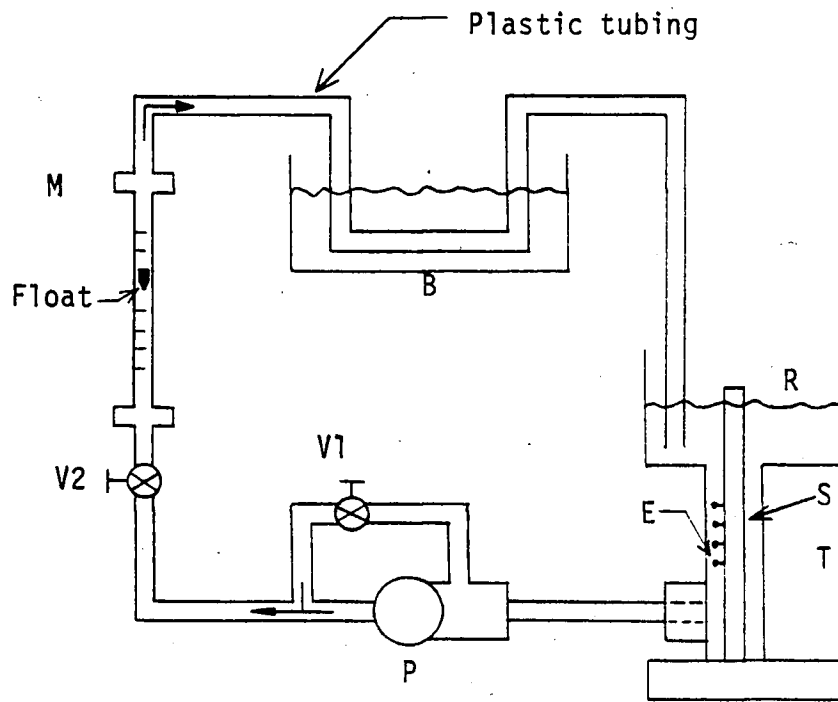
-29-

Fig. 12 - Mechanical setup of two probe experiment
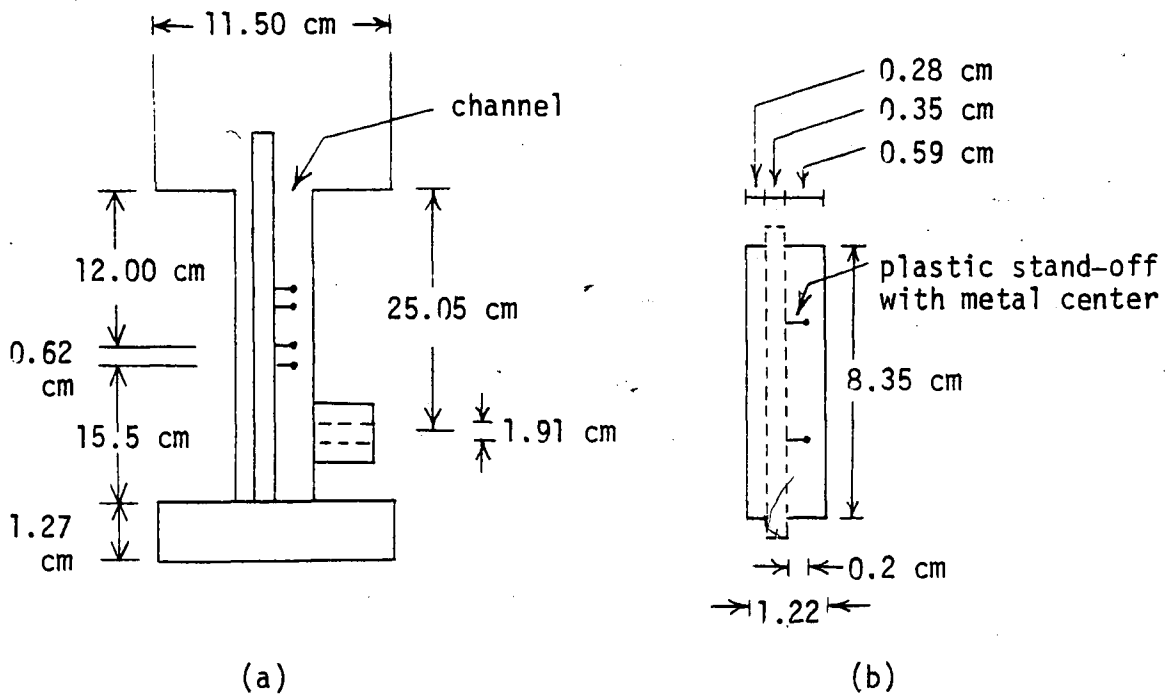
Fig. 13 - Pertinent dimensions of tower and sliding panel:
(a) front view of tower, (b) top view of channel,
probes and vicinity and (c) sliding plexiglass
panel with mounted platinum probes

-31-

of water volume to time recorded was the flow rate and the ratio of flow rate to the channel's cross-sectional area was the average velocity (cm/sec) in the channel. Since there is parabolic velocity profile in the channel ($v(x) = a-bx^2$ where x is measured from the center of the channel, compare Appendix A2), an analytical average velocity was calculated and set equal to the experimental average velocity in order to find "a" and "b" for each rotameter reading taken. With the position of the probes in the channel known ($|x|$ = 0.095 cm), the actual channel velocity at that position was then calculated for each rotameter reading taken. Finally, an interpolation was used to obtain values of the channel velocity at the probes for rotameter readings between those that were taken as data (see Appendix A2). The velocity at the probes ranged from 0.0 to 64.0 cm/sec. Rotameter data and calculations are given Appendix A2. It is noted that a velocity of 0 cm/sec corresponded to a rotameter value of -6 due to the rest-position of the float inside of the rotameter. For some measurements of current vs. velocity, the rotameter was replaced by a turbine flow meter having an electrical output (frequency and amplitude of a sine wave) proportional to the velocity of the solution passing through it.

Two dilute NaCl solutions were used. The first was 2.052×10^{-3} molar and the second was 4.104×10^{-4} molar - the former being of concentration five times that of the latter. These were produced by placing 5 ml and 1 ml respectively, of a 1.026 molar NaCl solution into the 2.50 litre system of deionized water. The error associated

-32-

with assuming the infinite dilution of these solutions is less than 5% (see Appendix A3) so that the theory presented on electrolytic conductance is applicable.

A circuit for the electrical setup is shown in Fig. 14. In most of the experiments, from among the four probes only two adjacent ones were used. Through a reed relay, a voltage source,
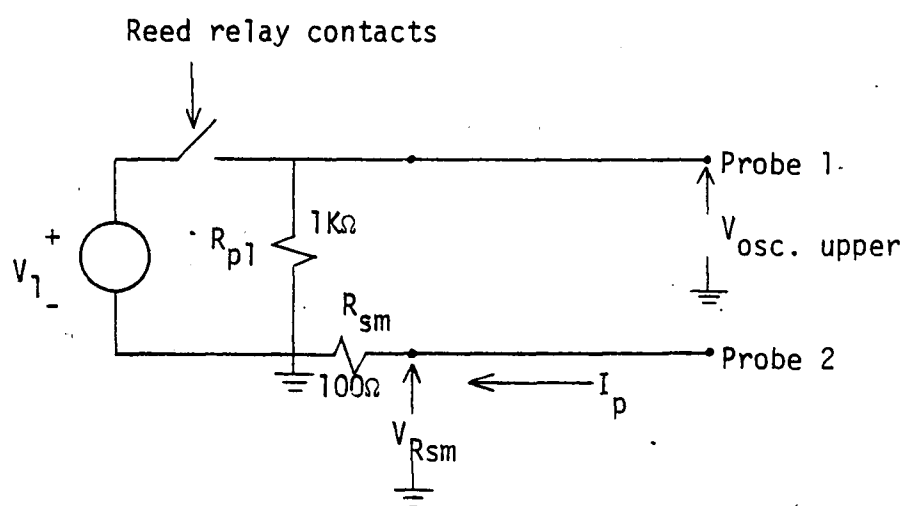
Fig. 14 - Two probe circuit

V_1, (used in both polarity configruations) was connected across R_{p1} (1kΩ). In series with the downstream probe was Rsm (100Ω±1%) which allowed the measurement of probe current, I_p (while droping an insignificant amount of voltage), during and after the application of a voltage pulse to the probes. The voltage from the first probe to ground, the source voltage, V_1, was observed on one trace of a storage oscilloscope while the voltage across Rsm, V_{Rsm}, was observed on the other trace. The relay was activated by a transistor switch and digital timing circuitry (see Appendix A4) with the

latter also generating triggering signals for the oscilloscope.

Data were taken on the relationship between the solution's velocity and conductance as a function of five different applied voltages, two concentrations (2.052×10^{-3} and 4.104×10^{-4} molar NaCl) and two temperature ranges (20-22°C and 40-44°C). Four experimental runs were made: The first was at the higher concentration and lower temperature, the second was at the same concentration but at the higher temperature, the third was at the lower concentration and lower temperature while the fourth run was done at the lower concentration and the higher temperature. For brevity these runs will be referred to as CT = 1,2,3 and 4 respectively. The solution of high concentration will be referred to as solution #3 and the solution of low concentration as solution #4. Starting at the lowest applied voltage, 2.01 v.d.c., and at the highest velocity, 64 cm/sec, a family of curves of V_{Rsm}(voltage across Rsm) vs. time, as a function of velocity (Fig. 15), were displayed on a storage oscilloscope and photographed with a camera. In turn, the voltage was increased to 3.01, 4.01, 10.01 and 15.05 v.d.c. while the same procedure occurred for each. After photographs were taken for CT = 1, the entire process was repeated for CT = 2,3 and 4. From these photographs the values of V_{Rsm} at t_0 = 3.2 sec (i.e. $V_{Rsm}|_{t_0}$) as well as the values of the positive and negative peaks were recorded corresponding to the appropriate conditions. Using a calibrated conductivity cell and an impedance bridge, the solution's conductivity was also measured

Voltage applied
to system
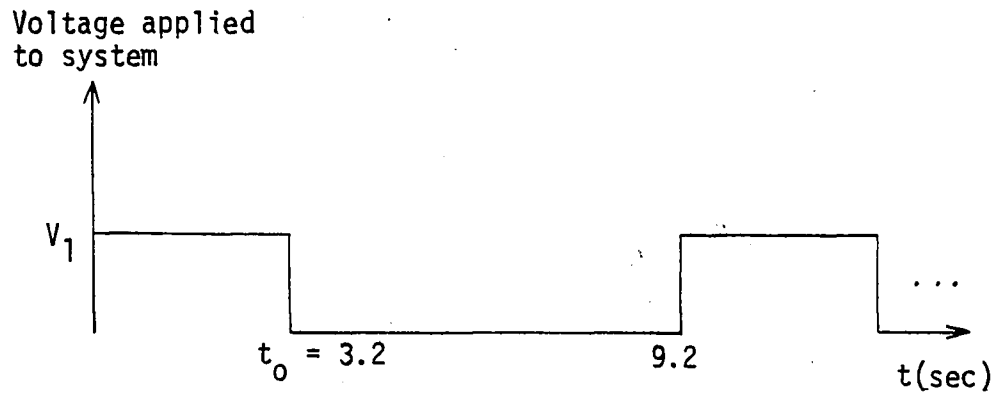
(a)
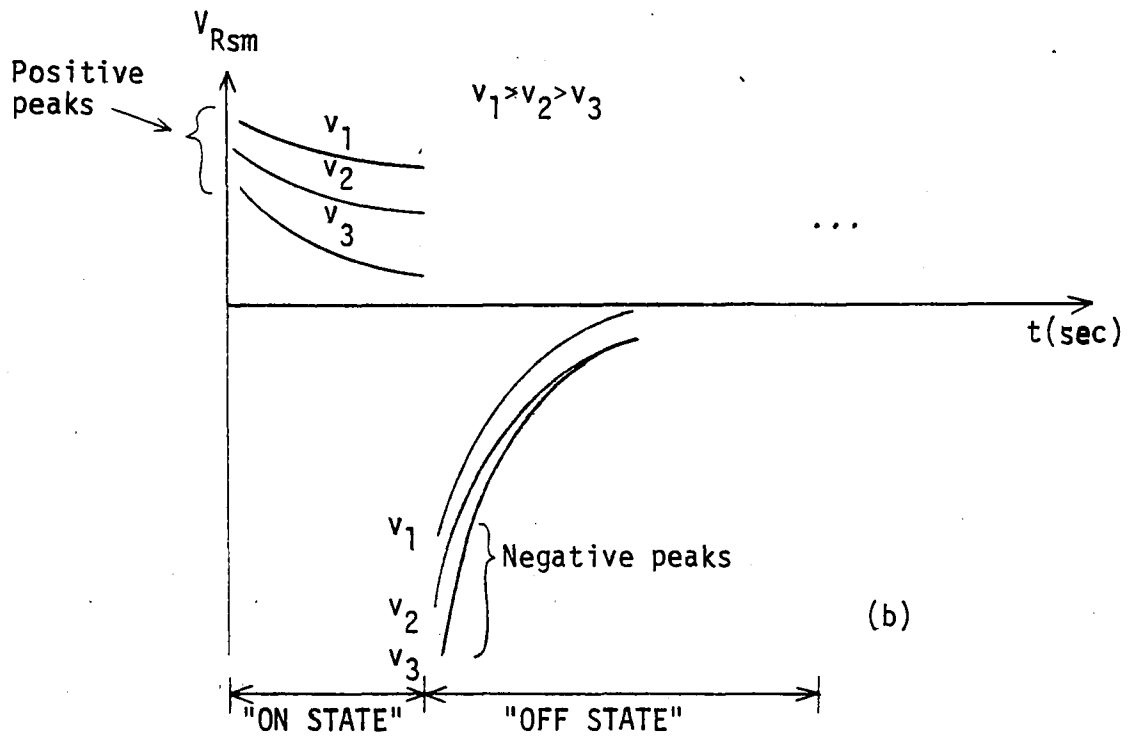
(b)

Fig. 15 - Illustration of waveforms: (a) voltage applied
to probes, (b) observed waveforms of V_{Rsm} as a
function of velocity

-35-

and recorded as a function of the solution's concentration and temp-
erature. The current through the probes, I_p, and the voltage across
them, V_p, both at $t = t_o$, can be expressed as

$$I_p\bigg|_{t_o} = \frac{V_{Rsm}\big|_{t_o}}{Rsm} \quad \text{and} \quad V_p\bigg|_{t_o} = V_1 - V_{Rsm}\bigg|_{t_o}$$

respectively. Therefore, the conductance between the probes is

$$G_p\bigg|_{t_o} = \frac{I_p\big|_{t_o}}{V_p\big|_{t_o}} = \frac{V_{Rsm}\big|_{t_o}}{V_1 - V_{Rsm}\big|_{t_o}}$$

Since the waveform of V_{Rsm} was approximately, if not completely hori-
zontal at $t = t_o$, I_p as given above is denoted as the "polarization
limit current" because the near zero slope is due to equal and
opposite values of $\vec{E}_{applied}$ and $\vec{E}_{polarization}$ (to be discussed
later). Since the phenomena observed were of an electrochemical
and electrolytic nature, conductance is a natural parameter and
hence will be computed and plotted in lieu of current. For each
value of CT, a plot was made of velocity versus conductance at t_o
as a function of the applied voltage V_1. Since polarity had little
effect on the observations, only the data corresponding to positive
values of V_1 were used and plotted.

3. POLARIZATION EFFECTS AT LOW VOLTAGES AND VELOCITIES

As described in Chapter 1 polarization builds up during a time interval after the onset of current. It results in a change in time of D.C. conductance between electrodes. Also, after the current has been turned off, a certain polarization voltage remains between the electrodes and only gradually (with a time scale measured in seconds) disappears. Therefore investigations of polarization effects have generally [10,11] been carried out with pulse techniques, observing the changes after turning currents on and off.

Naturally, if the electrolyte is moving, polarization charges will be removed as they build up. It is just this fact that gives some hope to be able to measure velocity from certain observations above polarization.

Therefore, we set up an experiment where the changes of current could be recorded after turning "on" and turning "off". If such records are made at different velocities, it can be hoped that some features in the time varying conductance or current could be reproducibly linked to velocity.

For that reason we constructed a circuit (see Appendix A4) that would automatically control the application of a voltage pulse (of predetermined amplitude), with respect to frequency and duration, across the pair of probes. For most of the relevant measurements, the pulse was present for 3.2 seconds and then absent for 6.0 seconds.

The cycle then repeated itself. Fig. 16 shows the circuit in semi-block diagram form. The circuit and as many wires as possible were placed inside a metal box - having feedthrough capacitors connected between itself and all leads entering it - to reduce noise pickup, especially from the pump motor which was in close proximity to all of the equipment.

Representative photographs of $V_{Rsm}(I_p = V_{Rsm}/Rsm)$ versus time, as a function of electrolyte velocity, for the four combinations of electrolyte concentration and temperature are shown in Fig. 17.[1] In all cases the absolute value of the current is observed to increase with velocity for both the "on" and "off" states of the applied voltage. This phenomenon will be called the low voltage or depolarization effect. Discussion and explanation of this effect will examine the charge movements of a sodium chloride solution both during and after a "low" voltage pulse is applied to the probes. For convenience the circuit is shown in Fig. 18 and the relevant waveforms in Fig. 19.

Zero solution velocity will be assumed for the present and hence for times less than t_1 the ions are randomly distributed (recall the strong electrolytic nature of NaCl resulting in complete ionization for dilute solutions). At $t = t_1$ the voltage pulse is applied and the charges begin to move in accordance with the equation, $\vec{F} = q\vec{E}_{net}$.

---

[1] Note that the voltage across Rsm and the voltage versus time curves are proportional to those of current, I_p, ($I_p = V_{Rsm}/Rsm$) and hence future discussions will refer to these curves as either current or voltage curves.

Therefore the chloride ions are attracted to the upper probe which is positively charged (the anode) while the sodium ions are attracted to the lower probe - both migrations contributing to I_p (Fig. 20 and Fig. 24. Charges congregate around the probes (Cl^- and Na^+ denoted as q_- and q_+ respectively) as time increases which causes two events to occur at approximately the same time. The first is the creation of an electric field of opposite direction to $\vec{E}_{applied}$ and is denoted $\vec{E}_{polarization}$. The second is the attraction and buildup of charges, in the probes, of opposite sign to that of q_- and q_+ (Fig. 20). These charges will be called $q_{+opposite}$ and $q_{-opposite}$, respectively. Essentially, $q_{+opposite}$ results from an absence of electrons in the anode. As time progresses, $\vec{E}_{pol}$ builds up and hence the net electric field, $\vec{E}_{tot} = E_{applied} + \vec{E}_{pol}$, will decrease (Fig. 21) thus causing I_p to decrease until $t = t_1'$ when a dynamic equilibrium is reached between the movement of charges due to $\vec{E}_{applied}$ and due to $\vec{E}_{pol}$. Therefore, when $V_{applied}$ is turned on, I_p reaches a peak value determined by the ratio of $V_{applied}$ and the resistance of the solution at that instant. As charges gather on the probes, a polarization field develops a shielding effect, which reduces the probe current until a steady state electric field is produced. The current remains at an equilibrium level, which is also called the polarization limit current (Fig. 19) for times between t_1' and t_2. When the voltage is switched off, i.e., for $t_2 \leq t \leq t_3$, the applied electric field becomes zero which means there is no external force holding q_- to the anode and q_+ to the cathode; however, the polarization field remains and thus accounts for the

total electric field for $t > t_2$ (Fig. 23). Therefore q_- and q_+ are attracted toward each other (Fig. 22) which reduces the attraction between q_{+opp} and q_- as well as that between q_{-opp} and q_+ (as does the fact that $V_{applied} = 0$) thus allowing q_{+opp} and q_{-opp} to flow toward each other in the probes and through Rsm. This last flow in addition to that of q_+ and q_- toward each other constitutes a current flowing in the opposite direction that I_p flowed, and is therefore denoted by "$-I_p$". Another illustration of the origin of $-I_p$ and its flow through the external loads is shown in Fig. 25. In short, at $t = t_2^+$, the only electric field present is $\vec{E}_{pol}$ which is due to the polarization charges, and because of its direction causes, as measured, a negative probe current to flow. As q_+ and q_- move closer to each other the magnitude of $\vec{E}_{pol}$ decreases and decays to zero, as does $-I_p$. It is also noted that the area under the positive and negative peaks of I_p is equal to the polarization charge since

$$\int I_p dt = q_+ = q_-$$

The restriction of zero velocity is now removed and the effects along with their causes are analyzed for increasing solution velocities. In the "on" state, as the solution's velocity is increased the q_- and q_+ ions are more readily removed from the probes, thereby reducing polarization effects and thus permitting the steady state current to increase. As stated before, $\vec{E}_{applied}$ equals zero in the "off" state and as such q_- and q_+ have no external force holding them to the upper and lower probes respectively. These ions will then be

attracted toward each other; however, as velocity increases more of the ions will be removed from the probe area, carried downstream, thereby decreasing their contribution to $-I_p$ and resulting in a reduced magnitude of $-I_p$.

Regarding the positive and negative peaks, the following is presented. Since the positive peaks depend solely upon $V_{applied}$ and the resistance of the solution at the moment of application of the voltage pulse, they should not vary with velocity - all other conditions kept constant (it is tacitly assumed that the conductance of the solution does not vary significantly at the velocities in question). However, since the solution is flowing when the pulse makes its on-to-off transition (and $\vec{E}_{applied} = 0$), the larger the velocity the greater the number of polarization charges that are washed away. In turn, the contributions to $-I_p$ are decreased which results in a smaller magnitude of the negative peaks. Summarizing these last two paragraphs we can say that during the "on" state, removal of the polarization charges increases the observed current (by decreasing the inhibiting forces) while in the "off" state, their removal decreases the magnitude of the observed current.

The photographs previously described indicate that velocity measurement is difficult at the low voltages which correspond to each combination of concentration and temperature. The reason is that in general there is not an adequate variation in the current curves as a function of velocity. This variation, however, spans a larger range

for high voltages than for low voltages as is shown in the next chapter. There are, nevertheless, some combinations of concentration, temperature and voltage, for which the photographs show exceptions to the above general statement. These are the photographs of CT = 1 for 2.01 volts and of CT = 2 for 2.01 volts which do have a relatively ample variation of current for different velocities (as is also born out by the conductance plots in Chapter 5). The word "relatively" means in comparison to adjacent curves of higher voltage. For example, for CT = 2, the curves for -2.01 volts (Fig. 17c) span velocities of 0 - 60.0 cm/sec over 14.5 mv while the ones for 3.01 volts (Fig. 26) span the same velocities, but only over 9 mv.
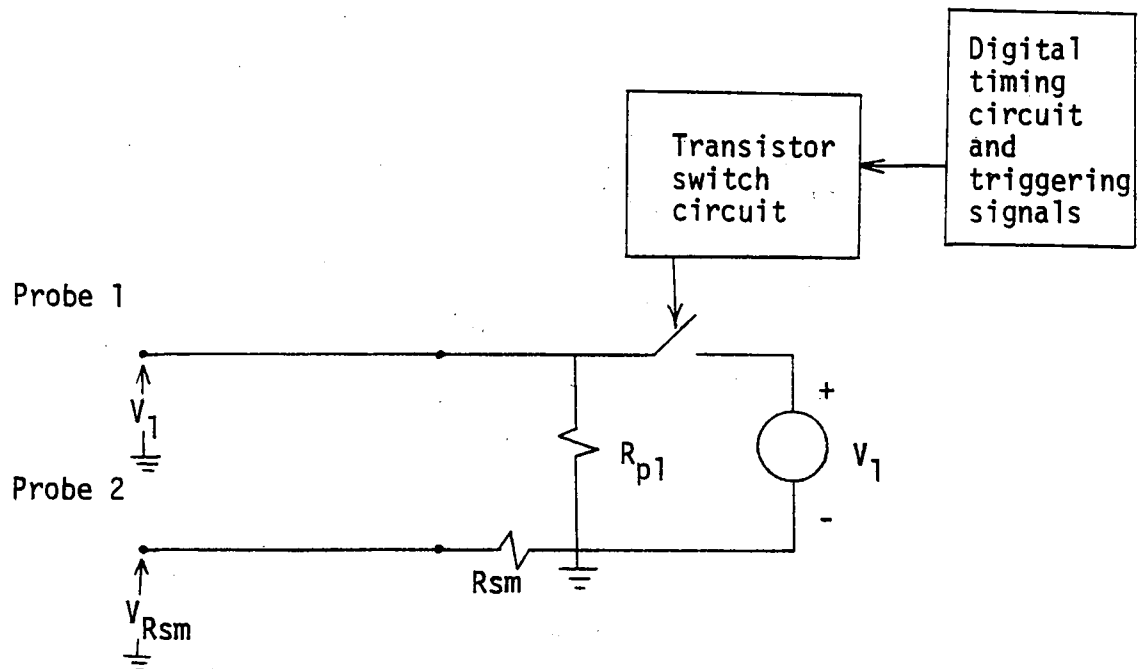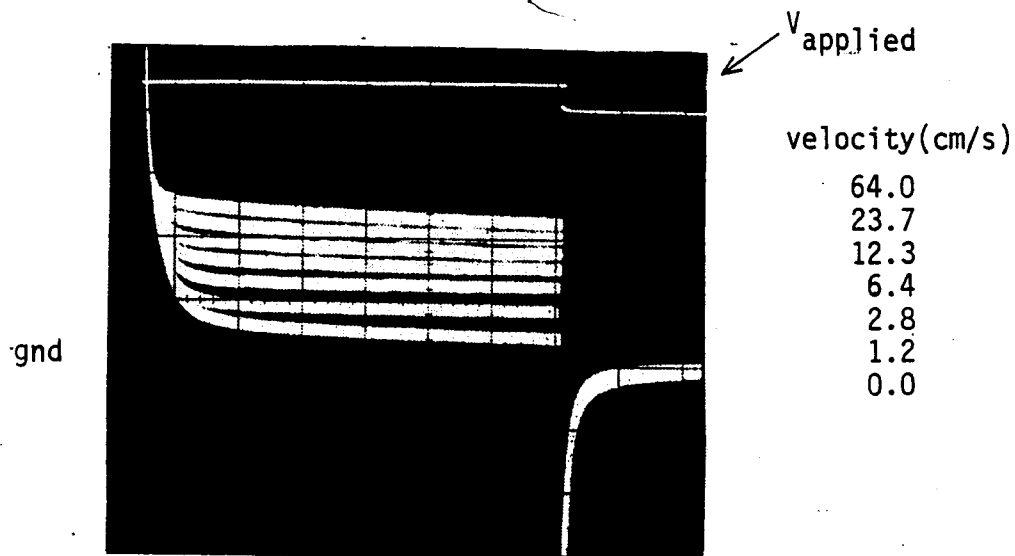
Fig. 16 - Block diagram and sketch of repetitive
          pulse application circuit

$V_{applied}$

velocity(cm/s)

| 64.0 |
| 23.7 |
| 12.3 |
| 6.4 |
| 2.8 |
| 1.2 |
| 0.0 |

gnd

(a)

| 64.0 |
| 47.8 |
| 31.0 |
| 19.1 |
| 8.8 |
| 2.8 |
| 1.2 |
| 0.0 |

gnd
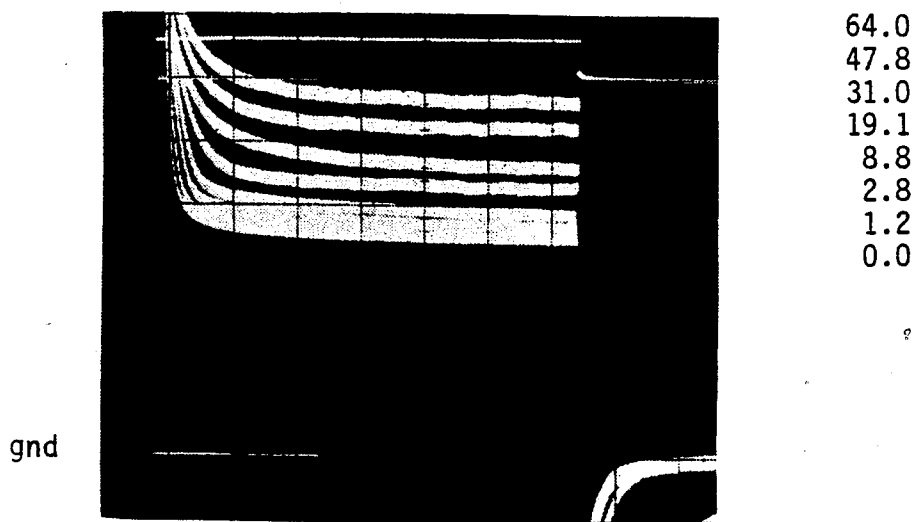
(b)

Fig. 17 - Photographs of V_{Rsm} vs. time as a function of velocity (low voltage)[1]. CT=1 for applied voltage and ordinate scale, respectively of: (a) +2v,5mv/div; (b) -3v,5mv/div

---

[1]Photographs are for applied voltages that give rise to the depolarization effect for various combinations of concentration, temperature and applied voltage. The abscissa has a scale of 0.5 sec/div. The trace of the applied voltage appears (with no scale) in the upper portion of some photographs. The abscissa, if present, is denoted by "gnd". "0.0(+8)" means a measurement was taken 8 secs after the solution stopped flowing.
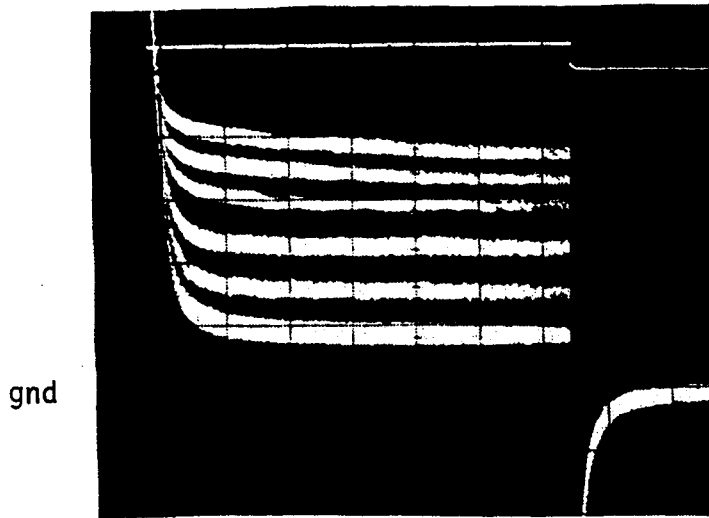
velocity(cm/s)

59.2
19.1
8.8
2.8
1.2
0.0

(c)
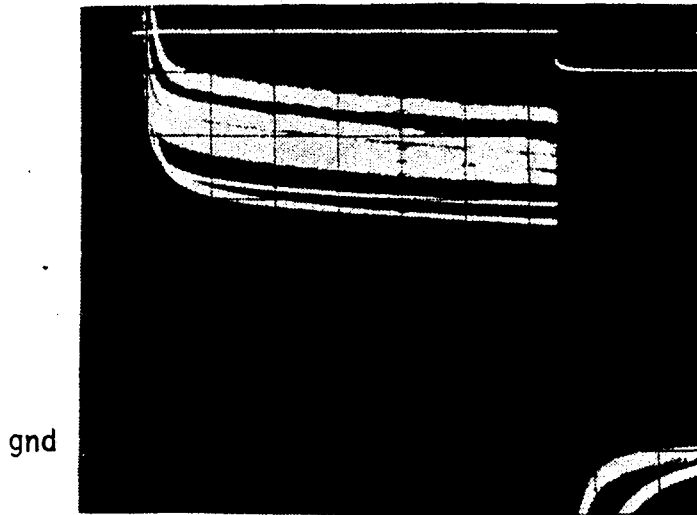
60.0
29.3
12.3
2.8
0.0
0.0(+8)

(d)

CT=2 for applied voltage and ordinate scale of:
(c) -2v, 5mv/div; (d) -3v, 5mv/div

gnd
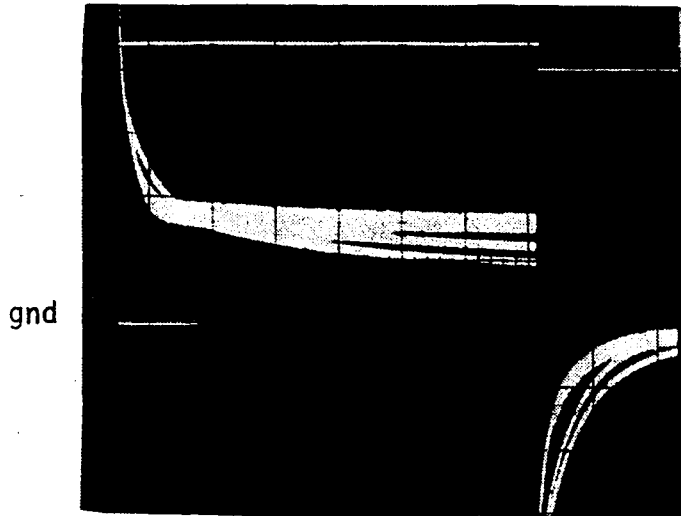
velocity(cm/s)
28.7
2.8
0.0
0.0(+8)
28.7
2.8
0.0
0.0(+8)

(e)

28.7
2.8
1.2
0.0(+8)
0.0

gnd
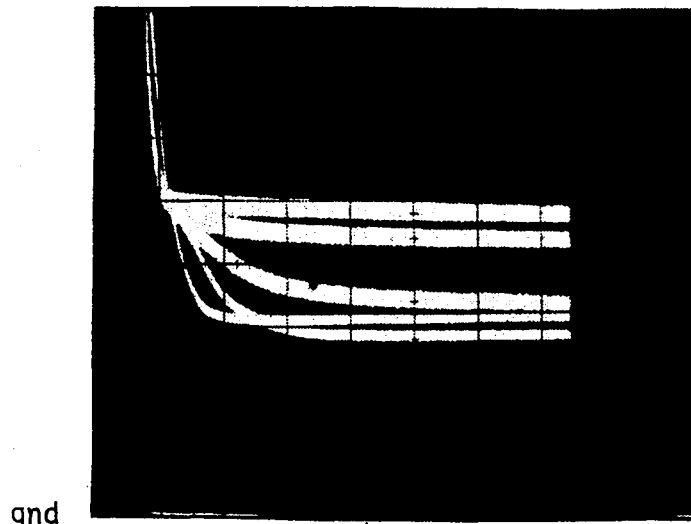
(f)

CT=3 for applied voltage and ordinate scale of:
(e) +2v, 2mv/div; (f) -3v, 2mv/div

velocity(cm/s)

28.7 6.4 1.2 0.0

gnd

(g)
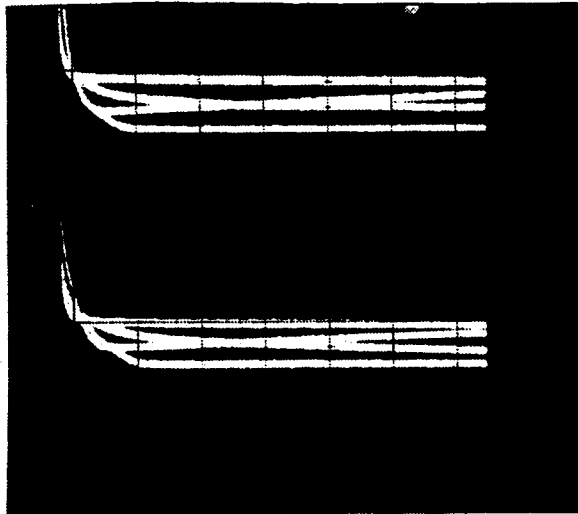
28.7 0.0 6.4 1.2

28.7 0.0 6.4 1.2

(h)

CT=3 for applied voltage and ordinate scale of:
(g) -4v, 10mv/div; (h) -4v(upper trace), +4v(lower trace),
5mv/div, ground is suppressed
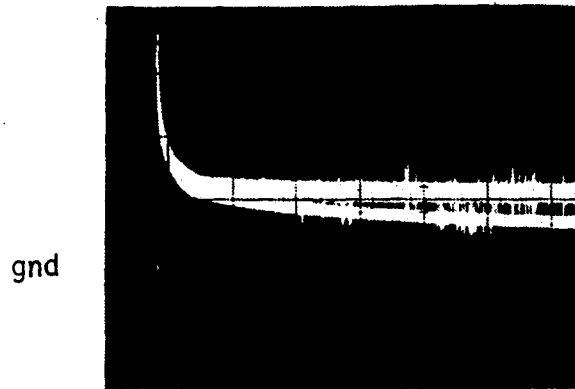
velocity(cm/s)

$^{59.2}$6.4$_{0.0}$

gnd

(i)

59.2
9.4
5.7
2.8
1.2
0.0

gnd

(j)
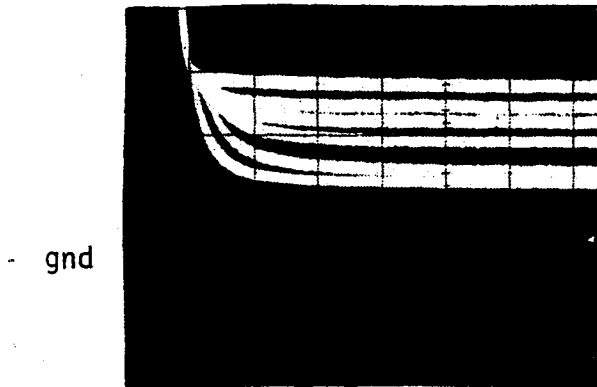
CT=4 for applied voltage and ordinate scale of:
(i) -2v, 5mv/div; (j) -3v, 5mv/div

-48-
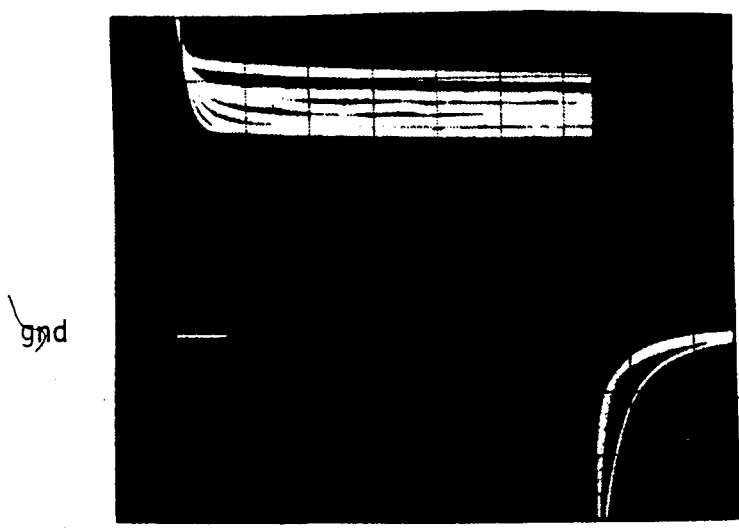
velocity(cm/s)

59.2
12.3
8.8
0.0
6.4
2.8

gnd

(k)

59.2
16.4
0.0
8.8
6.4
1.2

(1)
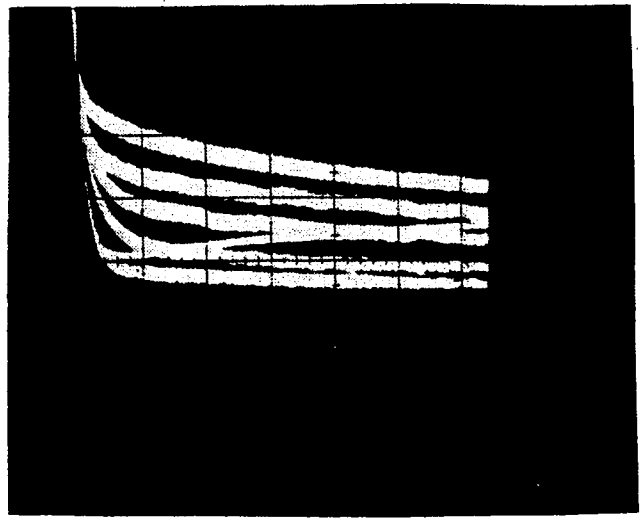
CT=4 for applied voltage and ordinate scale of:
(k) +4v, 5mv/div; (1) +4v, 2mv/div(ground is suppressed)
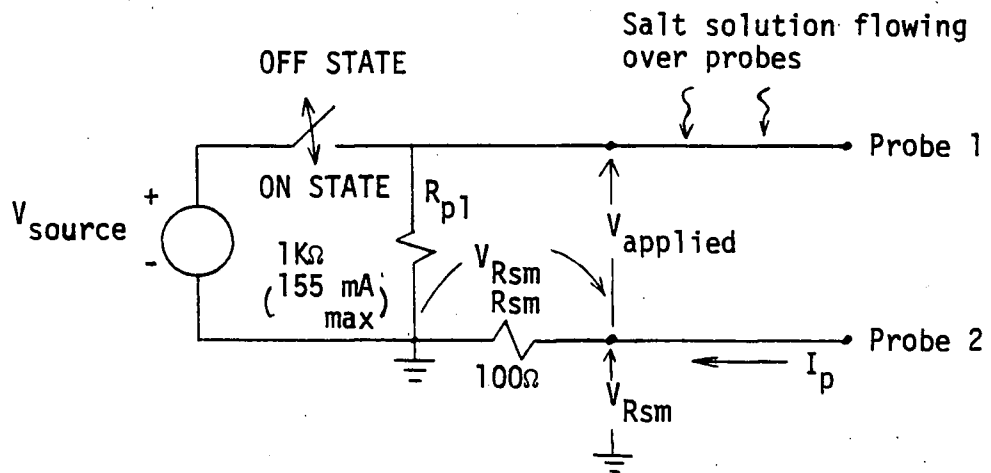
Fig. 18 - Circuit for conductance measurements.
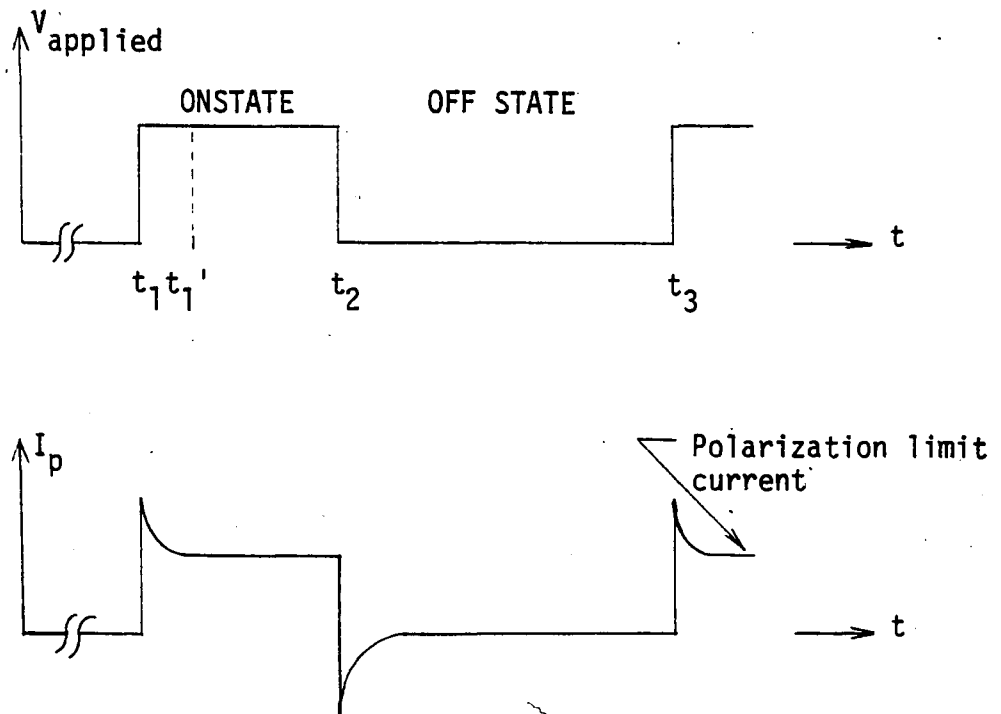
Fig. 19 - Applied voltage and observed current waveforms

-50-
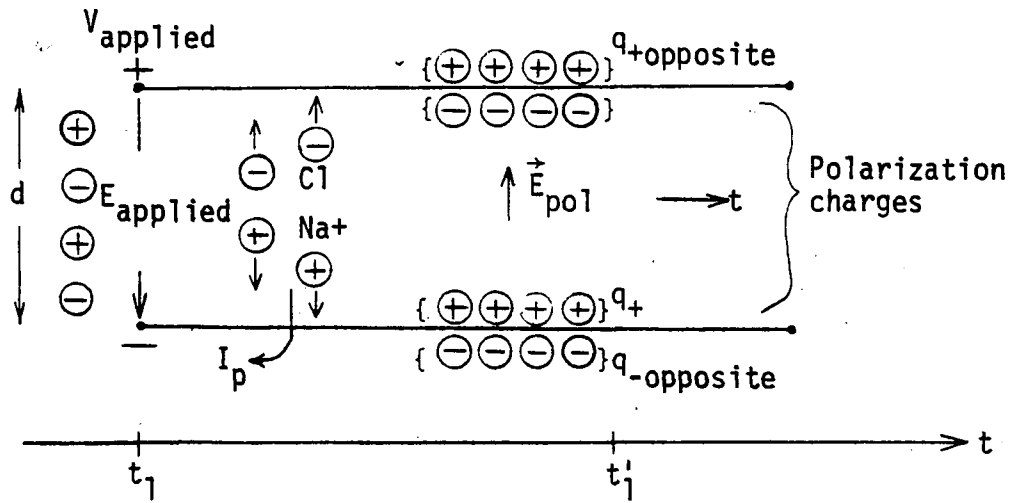
Fig. 20 - Charge distribute between probes
before and during voltage pulse
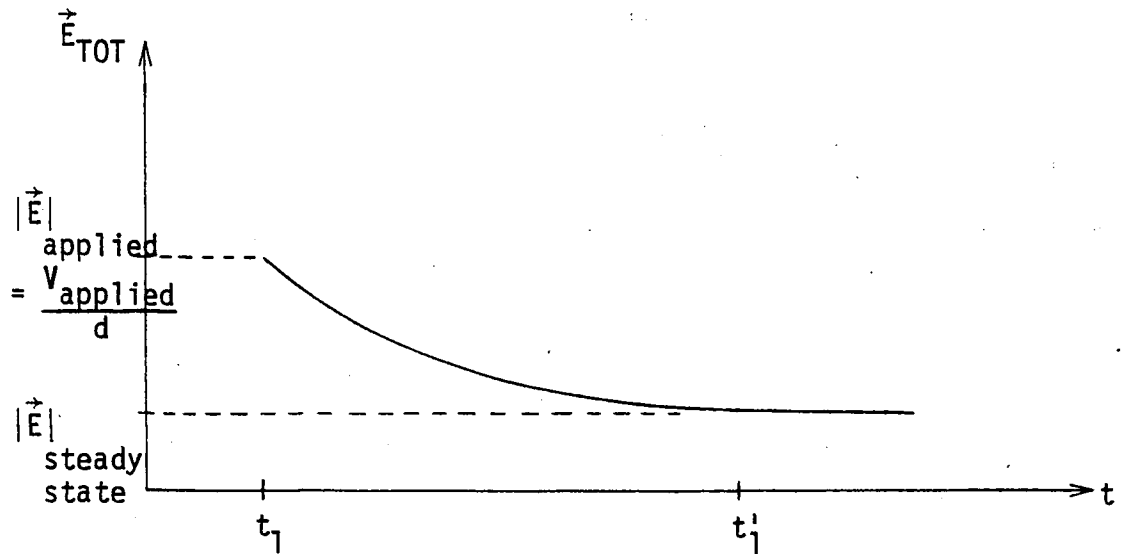
Fig. 21 - Electric field between probes
before and during voltage pulse

$$(|\vec{E}_{tot}| \alpha |I_p|)$$
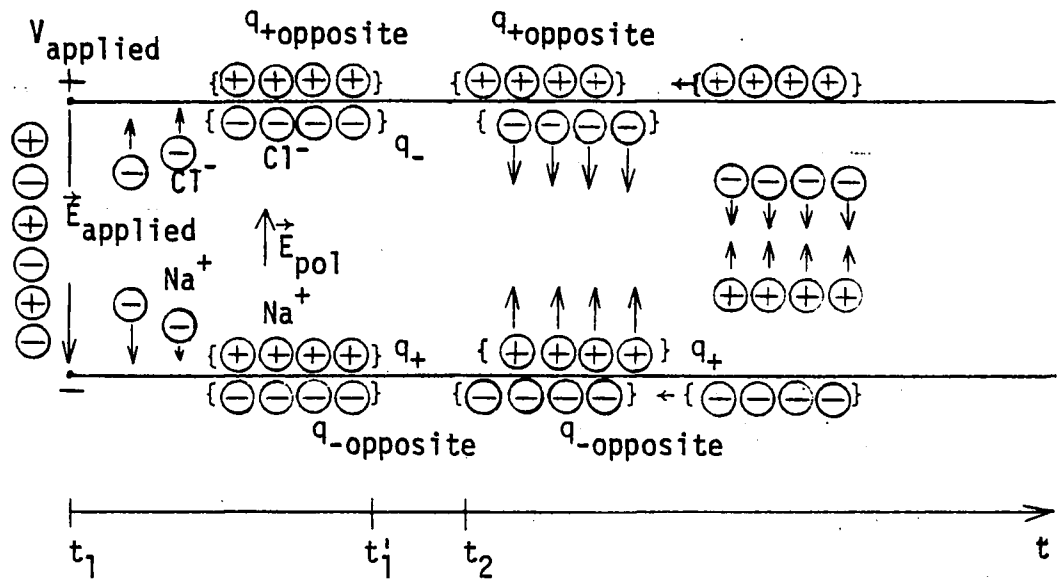
Fig. 22 - Charge distribution between probes before,
during and after application of voltage pulse
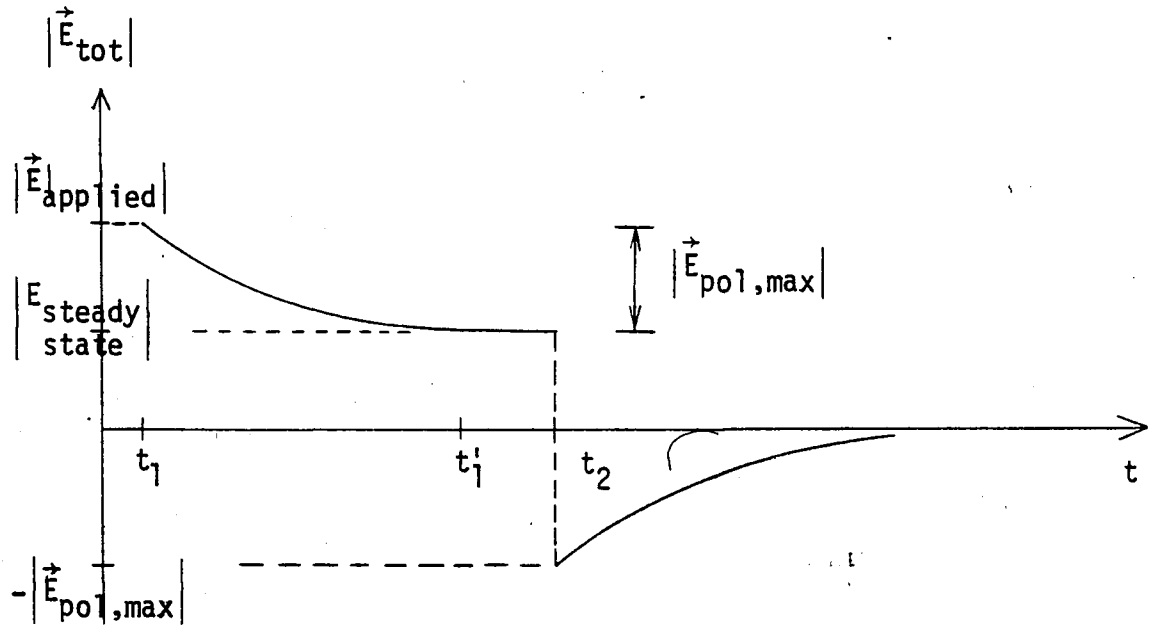
Fig. 23 - Electric field between probes before,
during and after application of
voltage pulse ($|\vec{E}_{tot}| \alpha |I_p|$)
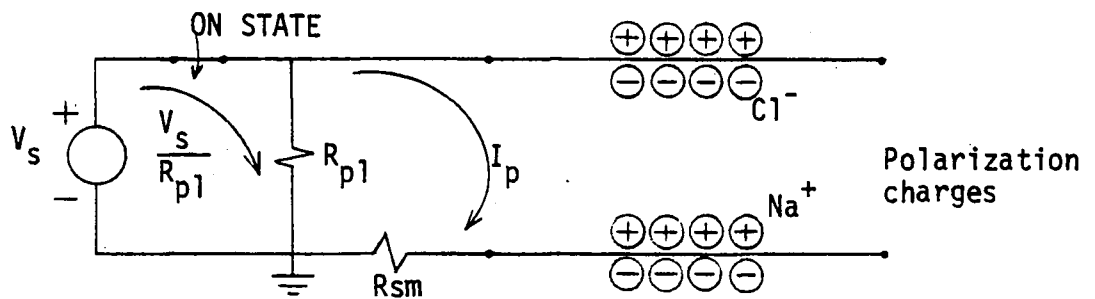
ON STATE

Fig. 24 - Attraction of polarization charges from
solution to the appropriate electrode
during the "on" state of V_s
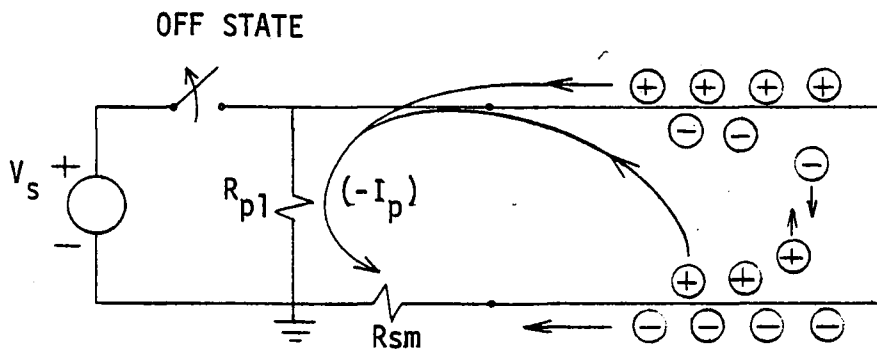
OFF STATE

Fig. 25 - Probe and polarization charges
contributing to the "off" state
current

velocity(cm/s)

58.4
29.3
15.8
6.4-0.0

58.4-1.2
0.0-0.0(+8)

Fig. 26 - Photograph of V_{Rsm} vs. time for CT=2, V_1= 3 volts; and a velocity range of: 0.0-58.4 cm/sec

4. CONDUCTANCE AT VOLTAGES ABOVE 3 VOLTS

As the measurements of the preceding chapter were extended to higher voltages it was noticed that surprisingly the current began to decrease as electrolyte velocity was increased, as shown in Figs. 27 and 28. This inverse effect cannot be explained with polarization since a buildup of charges always decreases the current in the absence of movement. In fact up to now, even with the large amount of literature on electrolytic polarization topics, we were not able to clearly understand the mechanism of this effect. An attempt to this end, however, is described in Chapter 6.

For voltages greater than those of Chapter 3, photographs of probe current ($I_p = V_{Rsm}/Rsm$) versus time with velocity, concentration and temperature as parameters are shown in Figs. 29. It is observed that as the applied voltage increases beyond the low voltage region (15, 10 and for some concentrations and temperatures, 4 volts) there is a range in which very little effect occurs: between 4 and 10 volts for CT = 1 and 2, and approximately 4 volts or less for CT = 3 and 4 (as will be better seen from the conductance plots in Chapter 5). Beyond this voltage range we were astonished to find an inverse effect: the magnitude of the current is observed to decrease as velocity increases. This is true during both the presence and absence of the voltage pulse. Because of this large variation, these photographs show better promise for a velocity measurement over those for low voltage as will be further discussed in Chapter 5.

velocity(cm/s)

$\swarrow V_{applied}$

64.0
23.7
12.3
6.4
2.8
1.2
0.0
0.0(after
9 seconds)

gnd

(a)

0.0
0.9
1.4
1.9
2.8
8.8
15.8
29.7
64.0

gnd
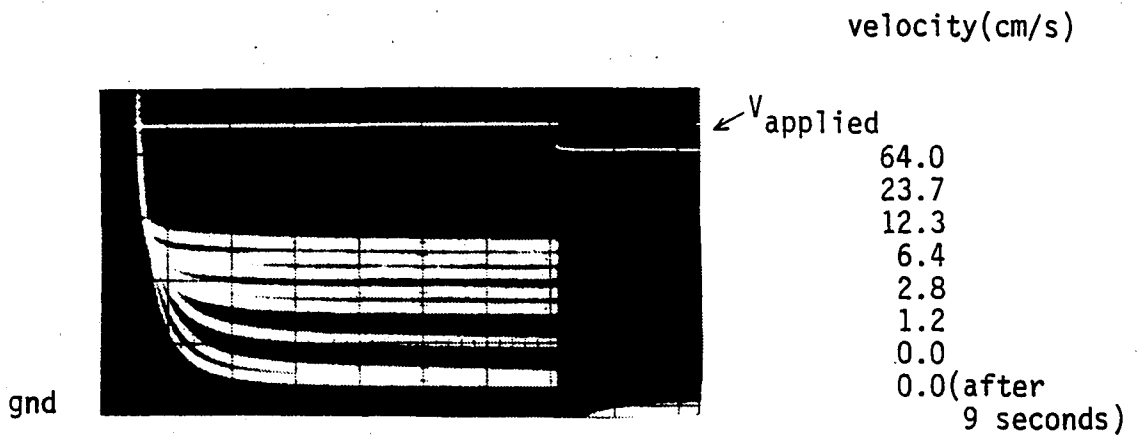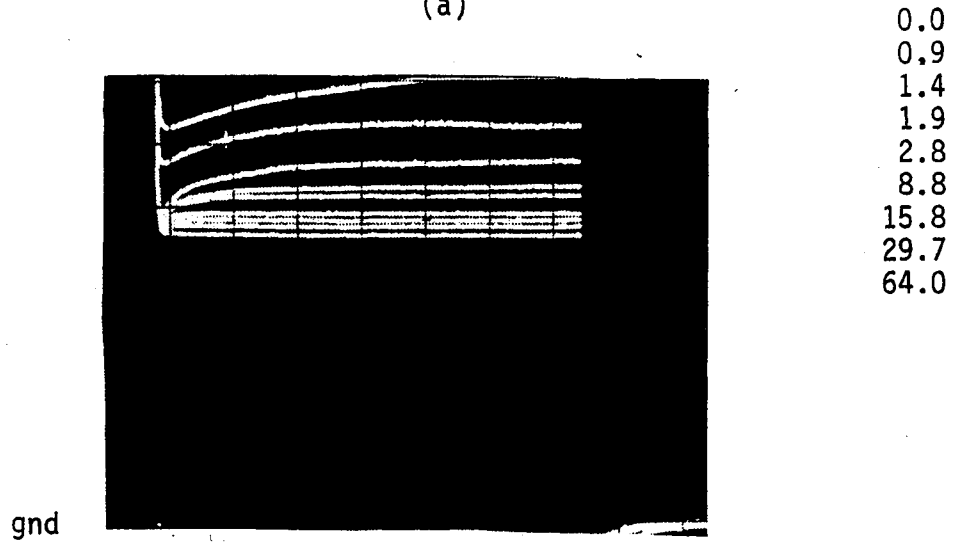
(b)

Fig. 27 - Voltage across R_{sm} vs. time as a function of
electrolyte velocity for CT=1:
(a) low voltage effect, $V_{applied}$ =-2v, 2mv/div, 0.5 sec/div;
(b) high voltage effect, $V_{applied}$ =+10v,50mv/div,0.5 sec/div
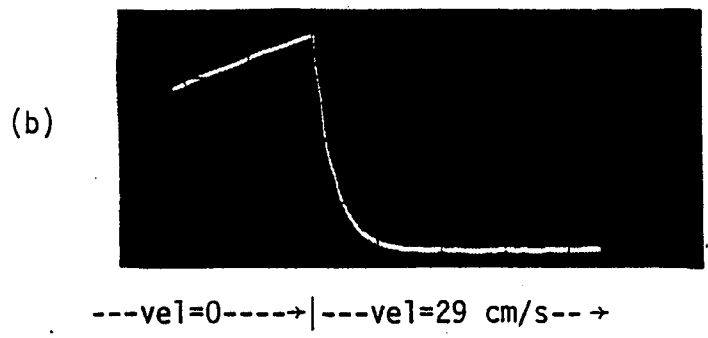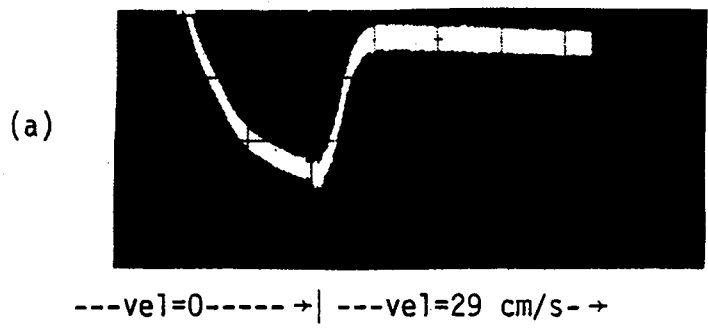
(a)

---vel=0----- →| ---vel=29 cm/s- →

(b)

---vel=0----→|---vel=29 cm/s-- →

Fig. 28 - Voltage across R_{sm} vs. time as electrolyte velocity increases from 0 to 29 cm/sec for CT=3. Ground is suppressed; 0.5 sec/div along abscissa:
(a) low voltage effect, V_1=+3v, 2mv/div;
(b) high voltage effect,V_1=-15v, 10 mv/div.

(a)

---vel=0----- →| ---vel=29 cm/s- →

(b)
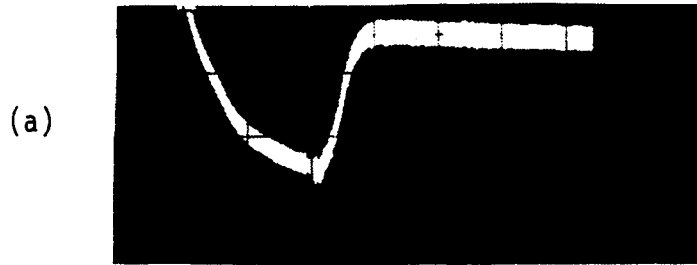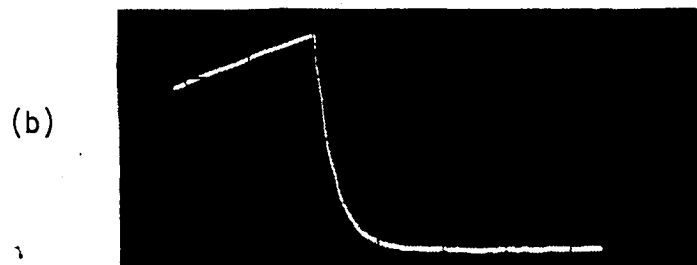
---vel=0----→|---vel=29 cm/s-- →

Fig. 28 - Voltage across R_{sm} vs. time as electrolyte velocity increases from 0 to 29 cm/sec for CT=3. Ground is suppressed; 0.5 sec/div along abscissa:
(a) low voltage effect, V_1=+3v, 2mv/div;
(b) high voltage effect, V_1=-15v, 10 mv/div.

velocity(cm/s)

(a)
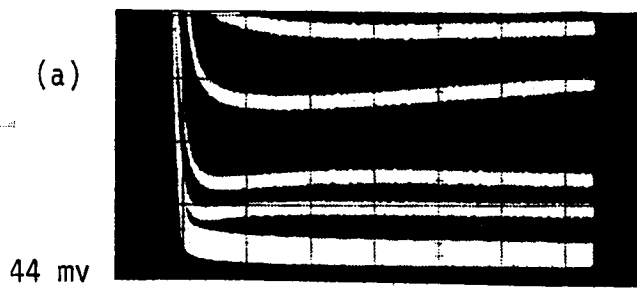
0.0(+8)
0.0

0.8

1.2
2.8
64.0
31.0-8.8

44 mv

0.0 0.7

1.2

1.9

6.4 8.8 2.8

15.8 29.7 64.0

(b)

gnd

0.0
1.2

2.8

12.3
31.0
64.0

(c)

gnd
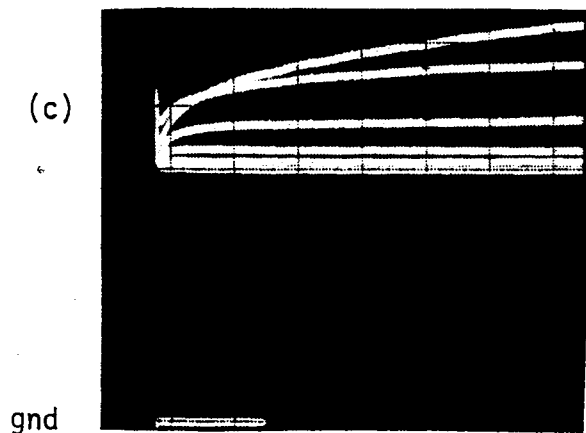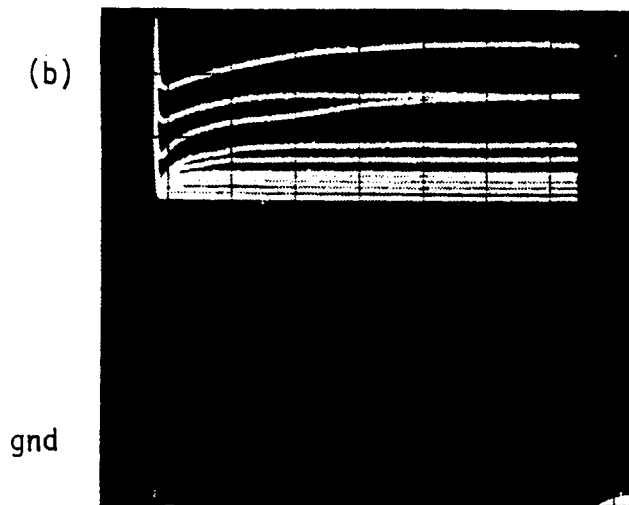
Fig. 29 - Photographs of V_{Rsm} vs. time as a function of velocity(high voltage)[1]. CT=1 for applied voltage and ordinate scale of: (a) -4v, 5mv/div; (b) +10v, 50mv/div; (c) -15v, 0.1v/div.

---

[1]Photographs are for applied voltages that give rise to the high voltage effect, for combinations of concentration, temperature and applied voltage. The abscissa has a scale of 0.5 sec/div.

velocity(cm/s)
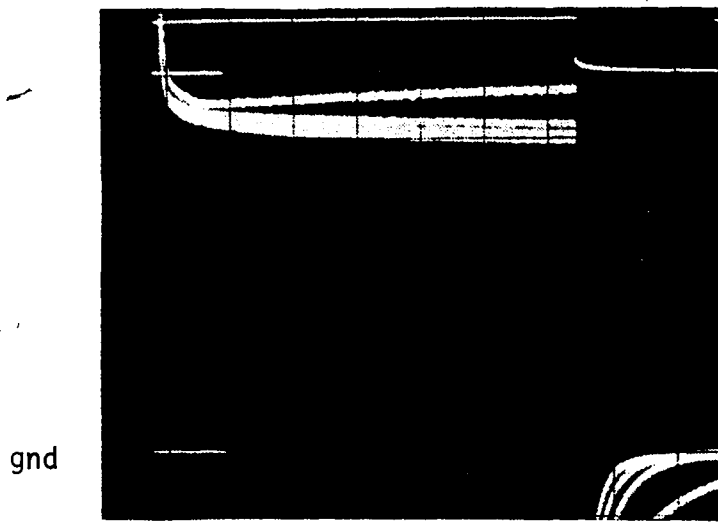
$V_{applied}$

0.0
1.2
2.8
29.3

gnd

29.3
2.8
1.2
0.0

(d)

1.2

2.8
6.4
8.8
14.5 29.3

.2 v

(e)

1.2
0.0
2.8
6.4
12.3
29.3

.4 v
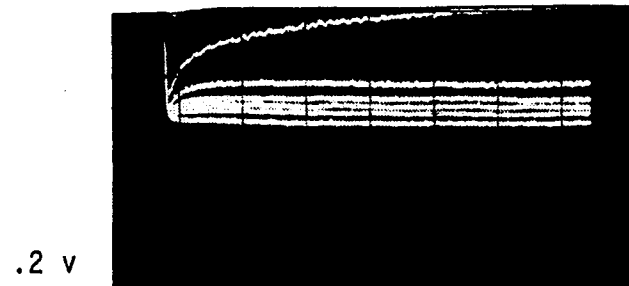
(f)

CT=2 for applied voltage and ordinate scale of:
(d) -4v, 10mv/div; (e) -10v, 50mv/div; (f) +15v, 0.1v/div
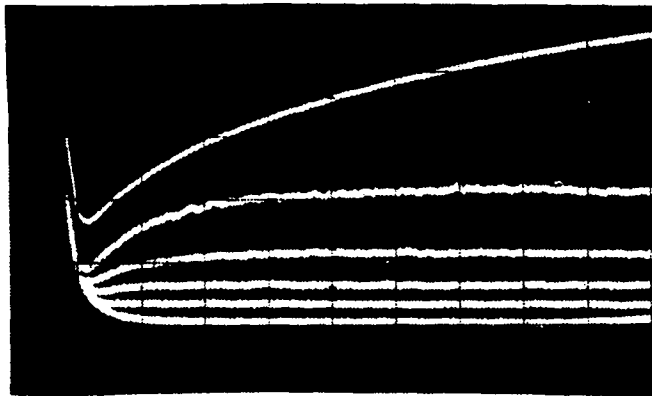
velocity(cm/s)

0.0

1.2

2.8
8.8
21.7
64.0

(g)
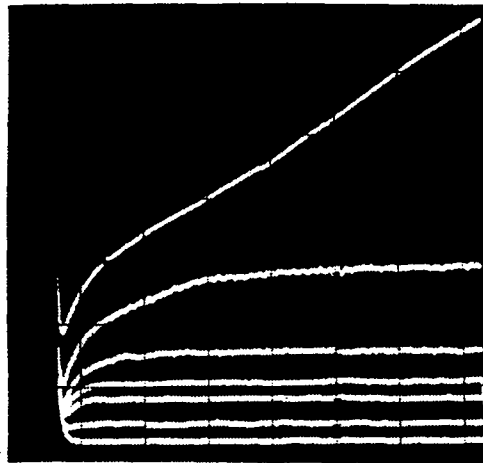
0.0

1.2

2.8

6.4
12.3
29.7
64.0

(h)

CT=3 for applied voltage and ordinate scale of:
(g) +10v, 5mv/div, 0.2 sec/div(ground is suppressed);
(h) +15v, 10mv/div, 0.5 sec/div(ground is suppressed)

velocity(cm/s)

0.0

1.2
2.8
6.4
12.3
19.1
59.2

gnd
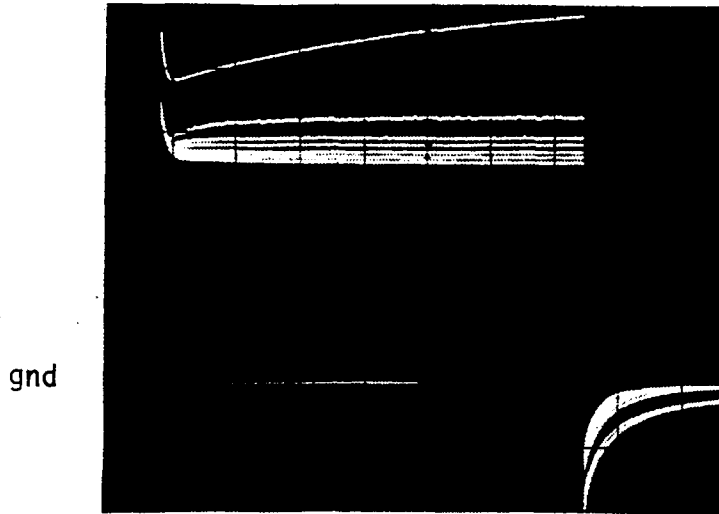
(i)
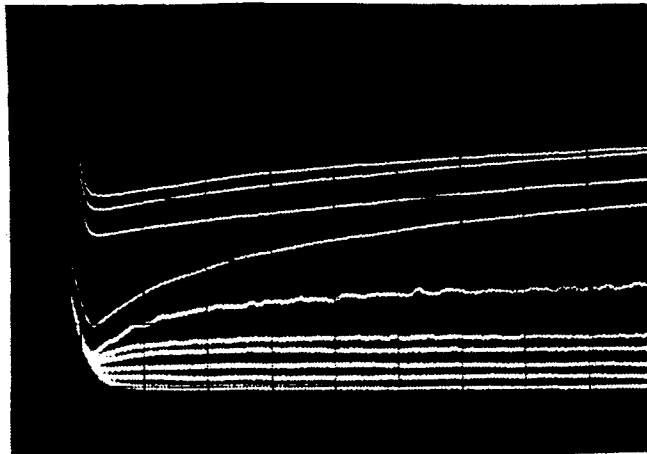
0.0(+24sec) 0.0(+16s)
0.0(+8sec)

0.0

1.2

2.8
6.4
12.3

19.1
59.2

(j)

CT=4 for applied voltage, ordinate scale and abscissa scale of:
(i) -10v, 20mv/div, 0.5 sec/div; (j) +10v, 10mv/div(ground is
suppressed), 0.2 sec/div

-61-
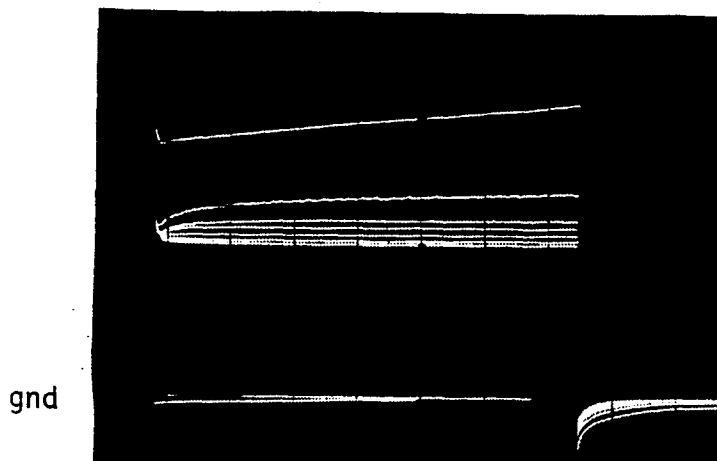
velocity(cm/s)

0.0(+8)
1.2
2.8
6.4 12.3 23.7 59.2

(k)

0.0(+8)

0.0

1.2
6.4 12.3 59.2

(1)
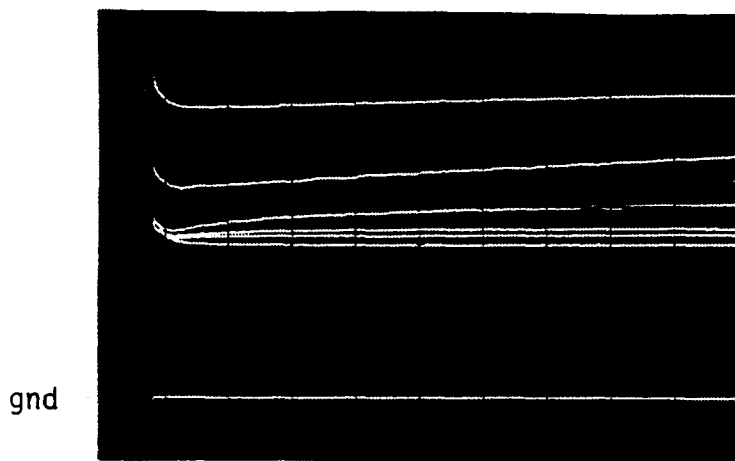
CT=4 for applied voltage of -15v, ordinate scale of 50mv/div
and abscissa scale of: (k) 0.5 sec/div; (1) 0.1 sec/div

5. DERIVED PLOTS OF VELOCITY VERSUS CONDUCTANCE

In order to obtain more detailed information on the relationship between the probe's conductance and the electrolyte's velocity, plots of velocity versus conductance were derived from the photographs. For each of the four combinations of electrolyte concentration and temperature, a plot was drawn of velocity versus conductance as a function of the applied voltages (2.01, 3.01, 4.01, 10.01, 15.04 v.d.c.) using only the data for the upstream probe being of positive polarity with respect to the downstream probe. The conductance between the probes was computed as the ratio of probe current to probe voltage. The former was obtained as the ratio of the voltage across Rsm at $t = t_0 = 3.2$ seconds (where the trace was not changing with time) to the value of Rsm (100 ohms) while the latter was equal to the difference between the applied voltage and that across Rsm. Referring to Fig. 14, the conductance between the probes at $t = t_0$ is expressed as

$$G_p\Big|_{t_0} = \frac{I_p\big|_{t_0}}{V_p\big|_{t_0}} = \frac{\dfrac{V_{Rsm}\big|_{t_0}}{Rsm}}{V_1 - V_{Rsm}\big|_{t_0}}$$

The semi-logarithmic plots are shown in Figs. 30a-30d followed by a detailed discussion of the data in both tabular and graphical form.

5.1 Discussion of Data

Examination of the characteristics of the measured data will

-63-
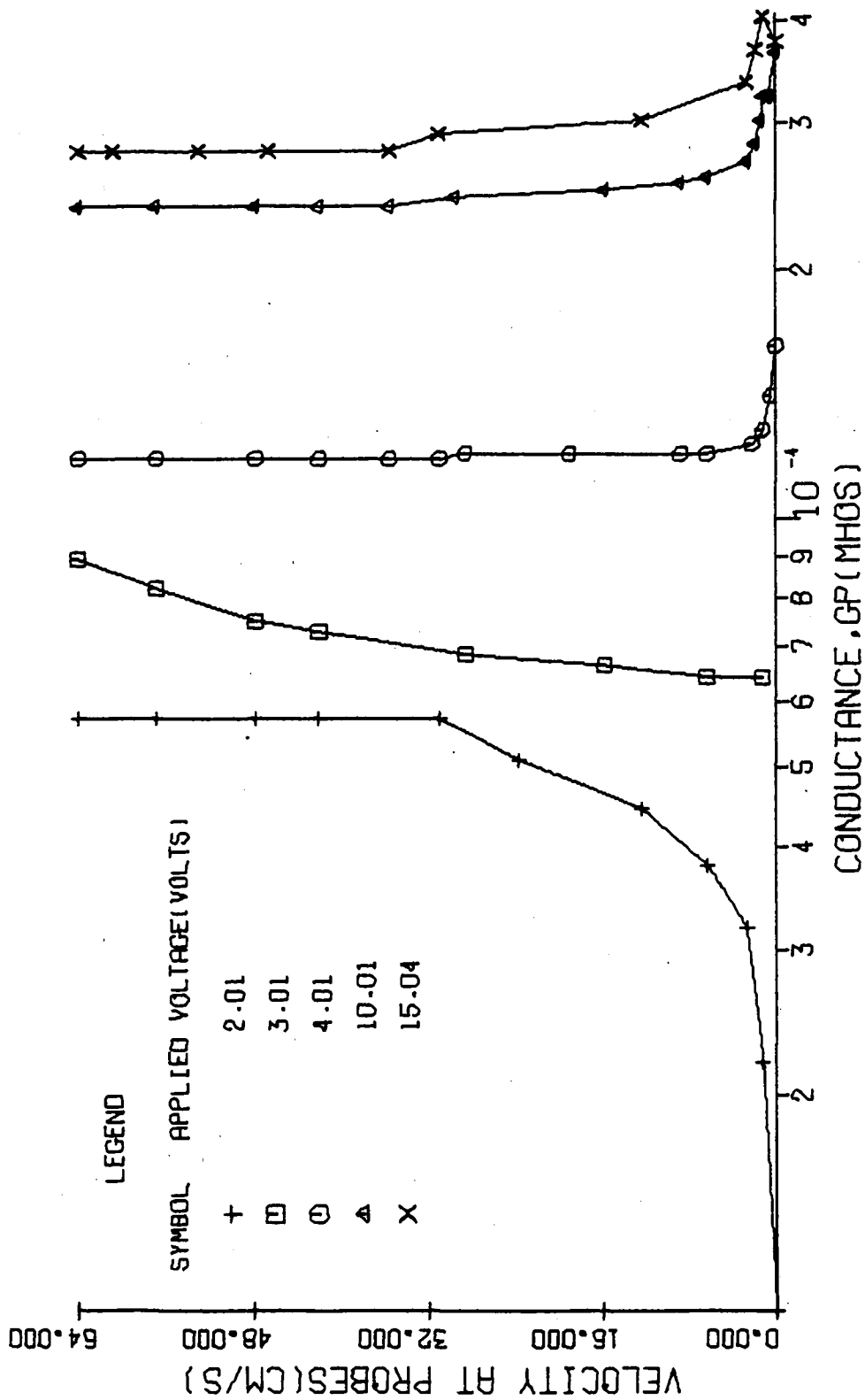
Fig. 30 - Velocity vs. probe conductance as a function of voltage for:

(a) high concentration, low temperature(CT=1)
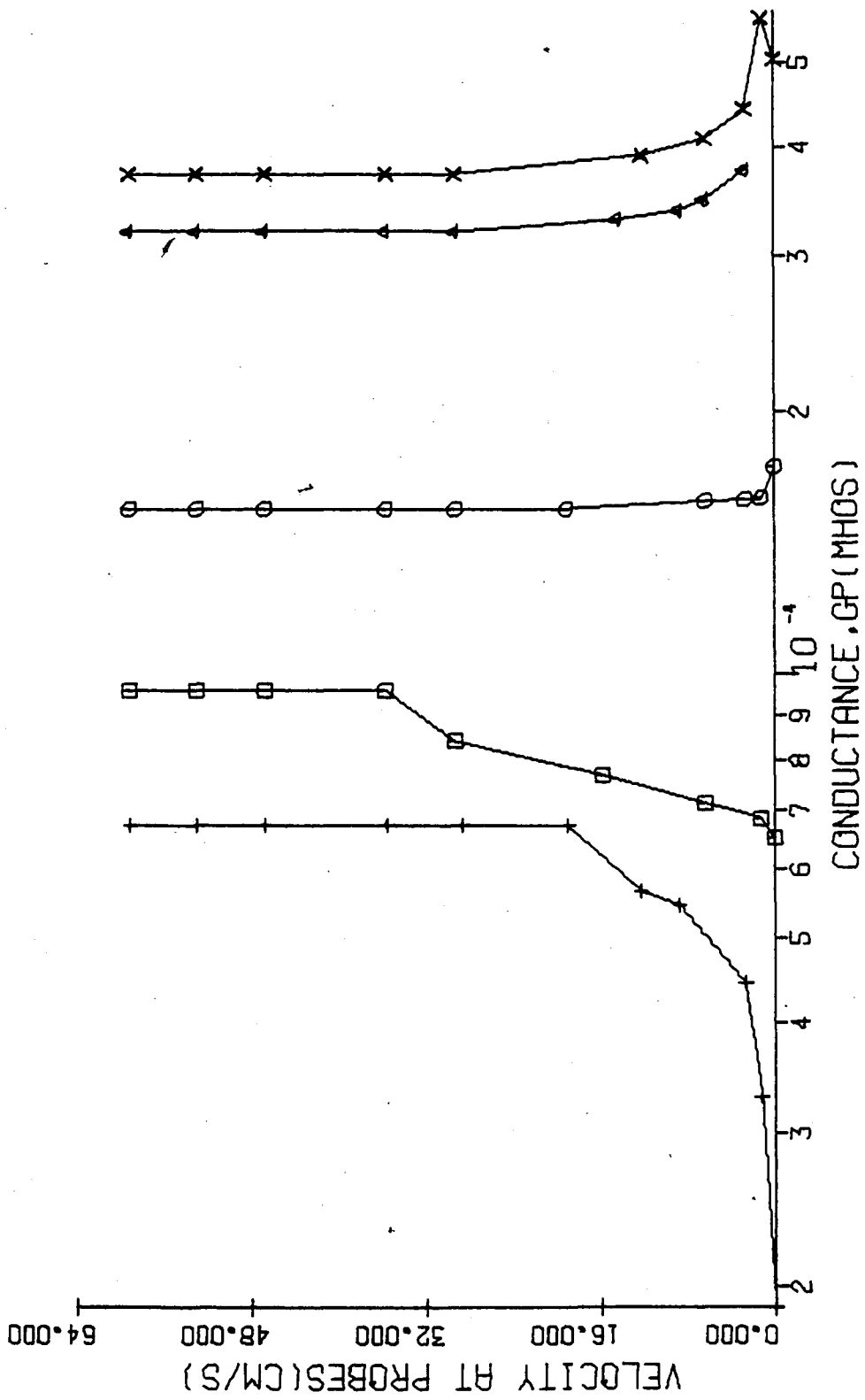
(b) high concentration, high temperature(CT=2)
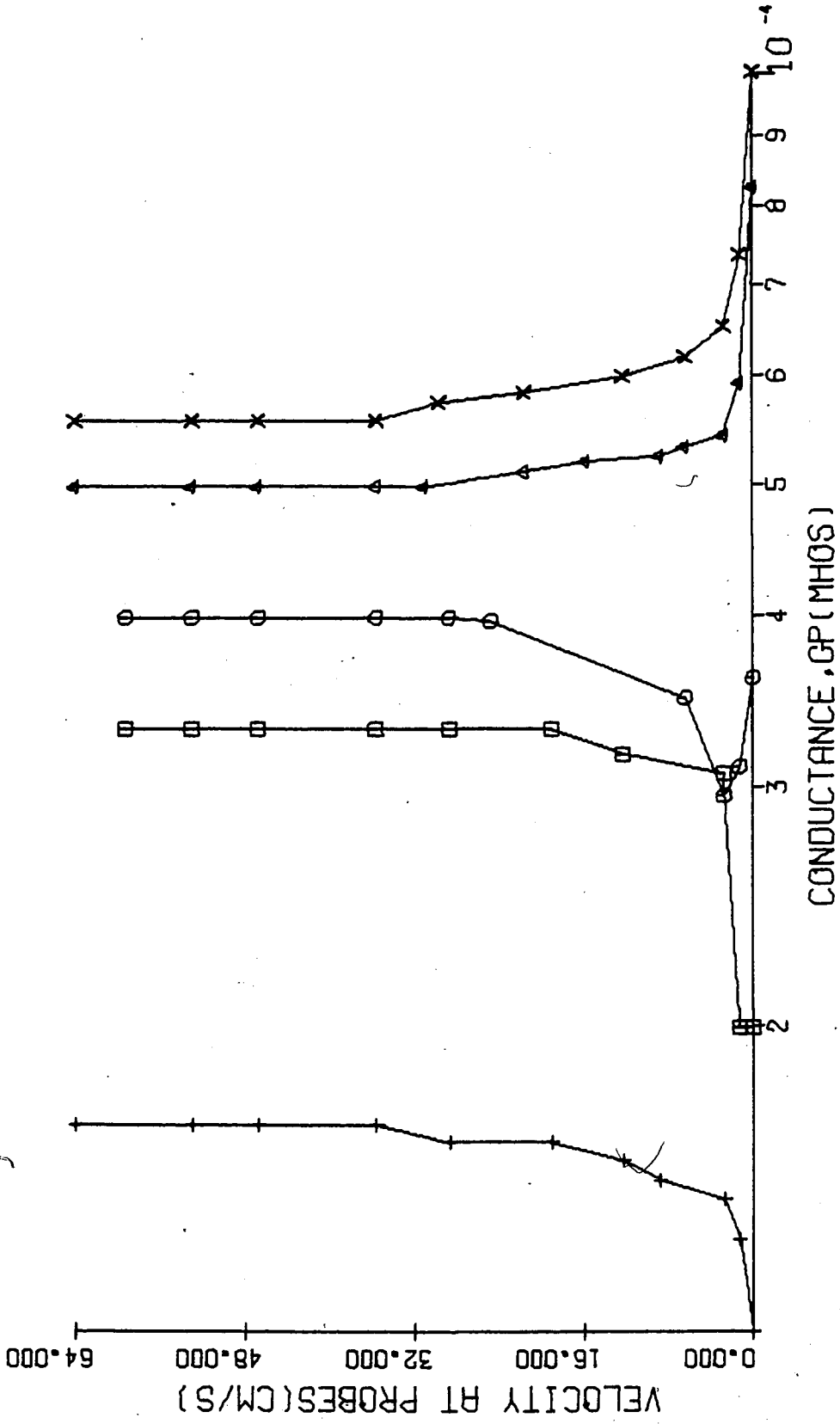
(c) low concentration, low temperature(CT=3).

-66-
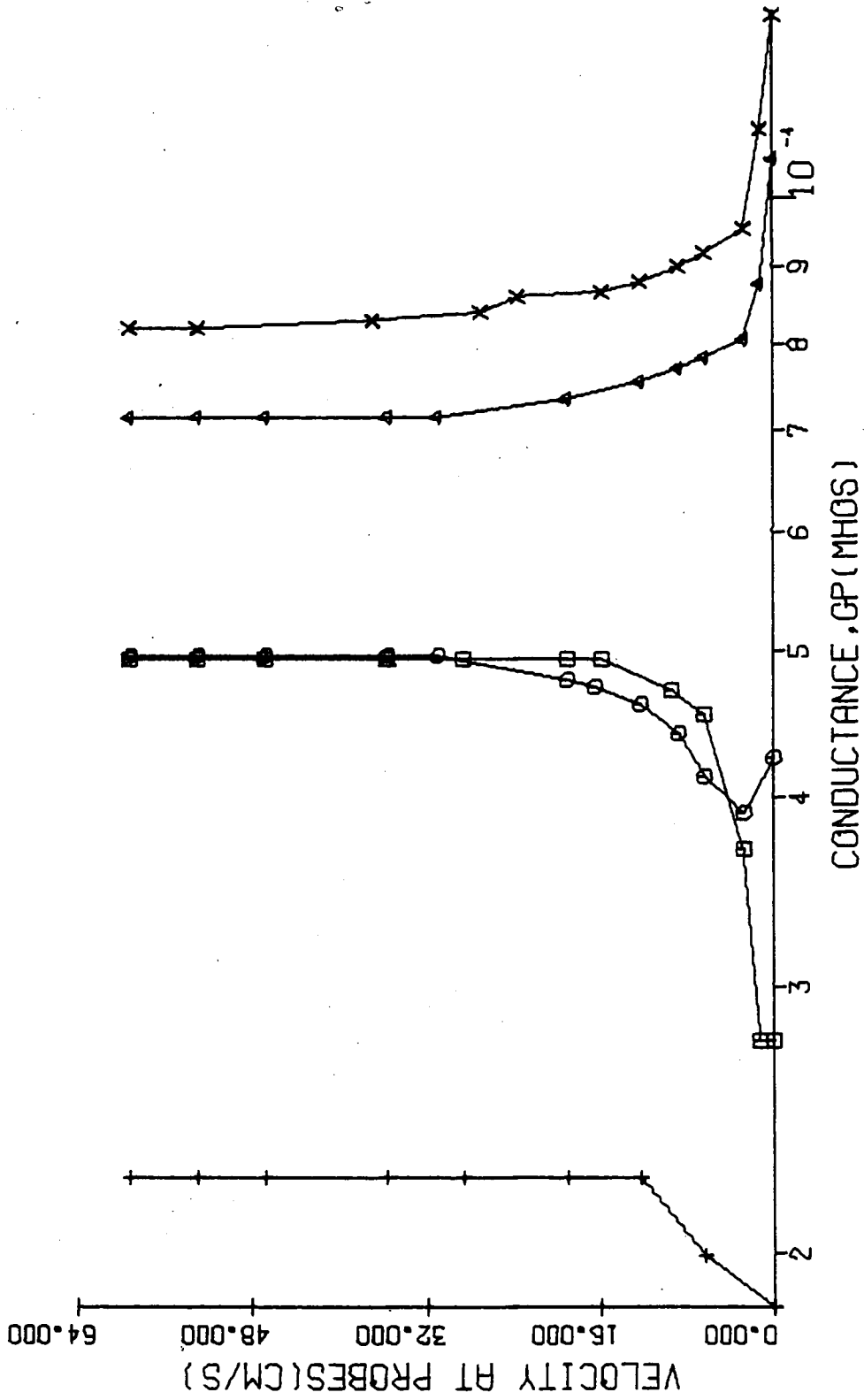
(d) low concentration, high temperature(CT=4)

make use of the data in tabular form as well as in graphical form.
It is noted that for applied voltages of less than 2 volts there were
no observable phenomena. As previously stated, polarity changes of
the probes had little or no effect on most observations of velocity
and conductance.

5.1.1 Tabular Form

Table II contains the measured conductivity of each solu-
tion as a function of the solution's temperature, concentration and
of the applied voltage. Since these measurements were performed using
a conductivity cell - a glass jar containing a sample of the solution -

TABLE II

Conductivity (x 10^{-6} cm^{-1} Ω^{-1}) As A Function Of Solution's
Temperature, Concentration And Of The Applied Voltage

Voltage (Volts)	Solution			
	CT=1	CT=2	CT=3	CT=4
±2.01	259.401	380.453	54.468	78.108
±3.01	265.227	379.383	54.962	78.445
±4.01	264.985	384.318	55.555	78.756
±10.01	264.401	378.431	55.026	78.481
±15.05	268.710	382.935	55.309	78.345

Average conductivity, with no regard for voltage

264.545	381.104	55.064	78.427

conductivity data were independent of the solution's velocity. It is
seen that variations in the applied voltage had little effect and
therefore an average conductivity was computed for each combination of
concentration and temperature. However, a proportional relationship,
which in fact is nearly a one-to-one correspondence, exists between

concentration and conductivity. The difference in concentration be-
tween solution #4 and solution #3 is a factor of 5 and the associated
change in average conductivity is a factor of approximately 4.8 and
4.86 for the low and high temperature ranges respectively. The data
also verify the increase in conductitivy of approximately 2.2% per
°C for salt solutions. Although the specific conductance at infinite
dilution, Λ_o, is the true quantity for which this variation holds,
the previous observation is valid because the comparison is made at a
concentration which is constant and approximately infinitely dilute.
In other words, the variation applies to Λ_o as well as to K, since
1000/C is a constant (recall the definitions: $\Lambda_o \overset{\Delta}{=} \lim_{c \to 0}$; $\overset{\Delta}{=} 1000K/C$).

While the relationship between concentration and conduc-
tivity (which included the parameters of voltage to a small degree
and velocity not at all) was almost a direct one, that between concen-
tration and calculated conductance at t_o was not direct in most cases;
although conductance is proportional to conductivity. Examination of
the tabulated data shows that increasing the solution's concentration
five times results in a variety of conductance increases for certain
velocities and applied voltages. Fig. 31 pictorially describes the
ranges and relationships of probe conductances, $G_p\big|_{t_o}$, (expressed in
mhos) according to the solution's concentration, temperature,
velocity and the applied voltage. It is noted that high velocity
means the maximum velocity attainable, 64.0 cm/sec, and that low vel-
ocity means 1.2 cm/sec. The reason that 0.0 cm/sec was not used for

Low Concentration

LOW TEMP

$V_1 = 2.01v$ $1.395 \times 10^{-5} \leq G_{p} < 1.694 \times 10^{-5}$ ——— x 1.57 (low velocity) ———

——— x 3.37 (high velocity) ———

$V_1 = 15.04v$ $5.549 \times 10^{-5} \leq G_{p} < 7.368 \times 10^{-5}$ ——— x 5.00 (high velocity) ———

——— x 5.48 (low velocity) ———

HIGH TEMP

$V_1 = 2.01v$ $\approx 1.9 \times 10^{-5} \leq G_{p} < 2.244 \times 10^{-5}$ ——— x 1.73 (low velocity) ———

——— x 2.99 (high velocity) ———

$V_1 = 15.04v$ $8.229 \times 10^{-5} \leq G_{p} < 1.109 \times 10^{-4}$ ——— x 4.53 (high velocity) ———

——— x 5.07 (low velocity) ———

High Concentration

$2.194 \times 10^{-5} \leq G_{p} < 5.704 \times 10^{-5}$

$2.774 \times 10^{-4} \leq G_{p} < 4.040 \times 10^{-4}$

$3.294 \times 10^{-5} \leq G_{p} < 6.711 \times 10^{-5}$

$3.724 \times 10^{-4} \leq G_{p} < 5.618 \times 10^{-4}$

Fig. 31 - Pictorial description of probe conductance under several conditions

the lowest velocity is that a measurement at zero velocity was found to be slightly dependent upon the duration of time that the velocity was equal to zero before a measurement was taken. For the high voltage range of 15.04 volts, at high and low temperatures and throughout the velocity range, a five fold increase in concentration resulted in an increase of $G_p\big|_{t_0}$ by a factor of 4.53 to 5.48. For the low voltage of 2.01 volts, at high and low temperatures and with a large velocity, the increase in concentration produced an increase of $G_p\big|_{t_0}$ by a factor of 2.99 to 3.37. With a low velocity and the same conditions, $G_p\big|_{t_0}$ increased by a factor of 1.57 to 1.73. Analysis of the above observations indicates that temperature was not a significant factor in the relationship between concentration and conductance. In addition, at high voltages, irrespective of the temperature, velocity and polarization effects, the chemical reactions at the electrodes occur so profusely that an increase in concentration of five times resulted in an increase of approximately the same amount. Although at a low voltage neither a large or small solution velocity resulted in approximately a five fold increase in conductance, at large velocities the data more closely represented a direct relationship. This may be explained by the removal of a buildup of current inhibiting charges as the solution's velocity increases - the depolarization effect.

5.1.2 Graphical Form

Perusal and discussion of the four velocity versus conductance graphs are best suited to be compared and contrasted by breakdown into three categories: (a) comparisons within a single

graph for which only the applied voltage changes, (b) comparisons of curves of different graphs for a given solution concentration and for a given voltage while the solution temperature is allowed to vary and (c) peculiarities or distinctions of an individual or general nature. It is worth noting that for graphs of a given temperature and varying concentration no specific remarks concerning comparisons can be stated. Again for brevity, CT = 1,2,3 and 4 will be used to refer to the conditions of high concentration-low temperature, high concentration-high temperature, low concentration-low temperature and low concentration-high temperature respectively. Also V_1 will denote the value of the applied voltage.

(a)   There are several significant points to be noted about the curves within a single graph. First, for CT = 4, the shapes of the curves for V_1 = 3 and 4 volts are very similar for velocities between 6.4 and 29 cm/sec while being almost identical for velocities between 29 and 64 cm/sec. For CT = 3 and V_1 = 3 and 4 volts, however, this observation is essentially absent. Within each graph (CT = 1,2,3 and 4), the curves for V_1 = 10 and 15 volts basically have the same shape-paralleling each other, just shifted in magnitude due to the differences in applied voltage from 4 to 5 volts. This fact occurs not only for a given graph, but the curves for V_1 = 10 and 15 volts are very similar for each combination of concentration and temperature - again just shifted due to the voltage difference. Another fact which is obvious from looking at each graph is that an increase in applied

voltage results in an increase in conductance. With conductance defined as $G_p = I_p/(V_1-V_{Rsm})$ an unobvious reason for this fact is that a certain increase in V_1 causes a greater increase in I_p, to which it is due. Electrode reactions occur at rates determined by many factors. One of these factors is the rate at which reactants are brought to the electrode's surface due to the stirring of a solution or due to a flowing solution. A proportional relationship between reaction rate and flow rate exists until this latter rate exceeds a certain value beyond which further increases in flow rate will not increase the reaction rate. Hence a limiting reaction rate is reached at and above this critical flow rate or velocity. With velocities as low as 12 cm/sec, this fact is substantiated by the asymptotic behaviour of conductance for all but one of the curves. The exception is for CT = 1 and $\dot{V}_1$ = 3 volts. The most conspicuous fact about each graph is probably the existence of a transition in the behaviour of $G_p\big|_{t_0}$ from proportional to inversely proportional as a function of voltage. The former characteristic is the depolarization effect, the latter the inverse effect. It is interesting to note that a semi well-defined transition occurs between 3 and 4 volts for CT = 1 and 2, while a less distinct transition occurs between 4 and 10 volts for CT = 3 and 4. The region of uncertainty is for velocities below 2.8 cm/sec. Therefore, it is the solution's concentration more so than its temperature which governs the voltage range in which the transition takes place.

(b)   When graphs of a given concentration and voltage are compared

-73-

in light of a varying temperature, three important points arise. The first is that an increase in temperature essentially shifts an entire curve to a greater conductance range without significantly changing the shape of the curve. This observation is explainable by the fact that the equivalent conductance at infinite dilution, Λ_o, of a salt solution increases by 2.2 - 2.5% for each increase in temperature of one degree Celsius. [12] The solutions that we used may be considered to have been at least 95% infinitely dilute (see appendix A3) and taking into account the fact that the comparison under discussion is for constant concentrations as well as the facts that conductivity, K, is proportional to conductance, G, and that $\Lambda_o \overset{\Delta}{=} 1000K/C$, the explanation is valid. The only exception to this observation is for CT = 1 and 2 with $V_1 = 3$ volts.

The second point to be made is that throughout the velocity range, there are remarkable similarities in the shapes of curves of the same concentration and voltage, but of different temperatures. For CT = 1 and 2, examples include the slow increase in conductance with velocity for V_1 = 2 volts; the slow decrease in conductance with velocity for V_1 = 4 volts for velocities below 2.3 cm/sec (CT = 1)and below 1.2 cm/sec (CT = 2); and the near identical arrow shape for V_1 = 15 volts and for velocities below 2.8 cm/sec. Again, the only anomaly to these similarities is for the 3 volt curve for CT = 1 and 2. It is noted, however, that this curve exhibits a monotonically increasing relationship between velocity and conductance and as such is considered part of the depolar-

ization curves. And for CT = 3 and 4, illustrations include the almost duplicate behaviour of the 3 volt curves for velocities below 2.8 cm/sec; the presence of a similarly shaped arrow for V_1 = 4 volts and for velocities below 6.4 cm/sec; the slow decrease in conductance with velocity for V_1 = 4 volts as well as 5 volts for velocities below 2.8 cm/sec for both voltages; and finally the sharp decrease in conductance with velocity for V_1 = 5 volts for velocities between 29.7 and 35.6 cm/sec (CT = 3) and for velocities between 23.7 and 27.0 cm/sec (CT = 4).

Table III illustrates the similarities between curves of the same concentration and voltage in velocity ranges larger than those stated above. The velocity at which an asymptote begins is also indicative of these similarities; the greater the velocity range over which two curves are asymptotic, the greater is their resemblance.

TABLE III.

Asymptotic Velocities

Velocities (cm/sec) at which asymptotes of velocity versus $G_p \bigg| t_0$ begin for each combination of concentration, temperature and voltage.

V_1:	2.01	3.01	4.01	10.01	15.04 volts
CT: 1	31.0	*	31.0	35.6	35.6
2	19.1	35.6	19.1	29.3	29.3
3	35.6	19.1	28.7	31.0	35.6
4	12.3	15.8	31.0	31.0	52.9

*No asymptote

The third point to note is that the 4 volt curves for CT =3 and 4 have the same property as do the 10 and 15 volt curves for velocities less than 2.8 cm/sec: decreasing conductance with increasing velocity. This may be indicative of the fact that the actual transition voltage is closer to 4 volts than it is to 10 volts. In contrast to all of the above similarities between curves is the fact that for CT = 3 and 4 (low concentration) the shapes of the curves for V_1 = 3 and 4 volts differ in the range of velocities greater than 6.4 cm/sec. For CT = 3, the curves are approximately parallel but separated after 6.4 cm/sec, while for CT = 4, as previously stated, the curves are parallel after 6.4 cm/sec and are almost coincident. We have seen therefore that variations in temperature do not alter the shapes of the curves nearly as much as do variations in con concentration.

Under the topic of varied characteristics of the data should be included the following obvious, unobvious and general observations. The obvious one is that although the curve for CT = 2 and V_1 = 4 volts has its asymptote beginning at a velocity of 19.1 cm/sec, there is an insignificant variation in $G_p\big|_{t_0}$ from 1.2 cm/sec up to 19.1 cm/sec. In other words, the conductance under the given conditions is almost constant throughout the upper 96% of the velocity range. No other curve exhibits this particular characteristic and, as such, would be unusable as part of a basis for a velocity measurement. This unvarying characteristic, however, may be indicative of the closeness of 4 volts to the actual turning point voltage between the depolarization and inverse effects.

-76-

An unobvious property of the data is the similar asymptotic values of conductance for several sets of curves as shown in Table IV

TABLE IV

Asymptotic Values of Conductance

Set #	Condition	Asymptotic Conductance (mhos)
1	$CT = 4$, $V_1 = 4v$	4.962×10^{-5}
	$CT = 3$, $V_1 = 10v$	4.960×10^{-5}
2	$CT = 2$, $V_1 = 10v$	3.196×10^{-4}
	$CT = 1$, $V_1 = 15v$	2.774×10^{-4}
3	$CT = 4$, $V_1 = 10v$	7.144×10^{-5}
	$CT = 2$, $V_1 = 2v$	6.711×10^{-5}
4	$CT = 2$, $V_1 = 4v$	1.545×10^{-4}
	$CT = 1$, $V_1 = 4v$	1.176×10^{-4}
5	$CT = 2$, $V_1 = 2v$	6.711×10^{-5}
	$CT = 1$, $V_1 = 2v$	5.704×10^{-5}

The conditions within set #1 and those within set #2 are of the same concentration but of different temperatures and voltages. The similar asymptotic values of conductance can be explained by the fact that the effect of a temperature decrease ($CT = 4$ to $CT = 3$), which causes a decrease in conductance, is counterbalanced by the effect of a voltage increase (4v to 10v), which causes an increase in conductance. The latter effect is seen in each of the velocity versus conductance graphs. Set #3 has conditions of constant temperature but of varying concentration voltage. Here, the resembling asymptotic values are due to the offsetting effects of an increasing solution concentration ($CT = 4$ to $CT = 2$) which increases conductance, and of a

decreasing applied voltage (10v to 2v) which decreases conductance. The data of set #3 are of uniform concentration and voltage but of different temperatures, an increase of which (CT = 1 to CT = 2) should result in a conductance increase. This hypothesis is supported by the data of set #4 as well as set #5.

One of the most general but distinct features of all the graphs is the presence of a shift in the values of the transition region from depolarization to inverse effects; from between 3 and 4 volts for CT = 1 and 2 to between 4 and 10 volts for CT = 3 and 4. Since the transition region is approximately the same for CT = 1 and 2 as it is for CT = 3 and 4, its origin appears to lie in the concentration differences, with little regard for temperature differences. As a sodium chloride solution's concentration increases, so does the number of sodium and chloride ions that are available for conduction. The corresponding increase in conduction decreases the resistance of the solution and hence lowers the voltage at which the transition occurs. Therefore, the shift is due to the decrease in required voltage (to start the inverse effect) for the solution of higher concentration.

Pointing out the three most prominent features of the velocity versus conductance graphs is in order. First is the striking resemblance of the curves for V_1 equal to 10 and 15 volts among all four graphs and in particular between graphs of the same concentration Second is the fact that there is an overall similarity in the shapes of the curves for a given concentration and voltage but for different

-78-

temperatures. And last, but the most salient of all features mentioned is the existence of two important effects in every graph: the depolarization effect for low voltages and the inverse effect for high voltages, where these voltage ranges are not clearly distinguisable and are separated by a transition region which is dependent upon several parameters.

5.2 Remarks Regarding A Velocity Measurement

A method for flow measurements is one in which a two probe apparatus is used in conjunction with a previously calibrated data table. The data table is calibrated for that particular probe configuration immersed in an electrolyte-carrying channel of given dimensions, for solutions of known concentration and temperature and for known applied voltages whose pulse widths are of sufficient duration to yield a fairly constant value of probe current, i.e., a steady state is reached. Measurements of conductance are recorded and the corresponding velocity is looked up in the table.

Considering the range over which the velocity versus $G_p\big|_{t_o}$ curves are generally and smoothly monotonic, a velocity measurement is, in general, better when performed at the higher voltages rather than at the lower ones. Using the above criterion as a figure of merit, we found a velocity measurement reliable for velocities up to 31-36 cm/sec under optimum conditions, such as conductance curves exhibiting significant change for increasing velocity. Accordingly, the curves for $V_1 = 10$ and 15 volts of CT = 3 are the ones best

suited for a velocity measurement. Linear plots more closely verify the previous statements; however, semi-logarithmic plots were necessary for purposes of physical space restrictions. Although limited in range and applicability, under the conditions stated heretofore and utilizing velocity-dependent conductance relationships, a velocity measurement is possible.

6. ON THE MECHANISM OF THE HIGH VOLTAGE EFFECT

Recall the discussion of electrolyzing a salt solution in Chapter 1. Accordingly, a hypothesis of the mechanism governing the inverse effect was proposed and tested, which involved some of the chemical reactions at the surface of the anode. One of the reactions on the anode is the formation of HCl from Cl_2 and water. This reaction necessarily takes place since it is H_2 that is released and not Cl_2. Also the said reaction does not occur spontaneously if Cl_2 is dissolved in water. We conclude that the surface of the platinum wires is involved. Also one could say that if the Cl_2 is washed away before it has time to react there would be a loss of conducting ions, namely the H^+ after HCl has dissociated. That would explain the decrease of current with increasing velocity.

To investigate the above hypothesis the following test was performed: The probe that was most downstream - of a horizontal, three probe configuration - was covered with filter paper conforming to the shape of a tent. In this way the velocity near the platinum surface was effectively reduced to zero. Current versus velocity measurements were taken using the upper and middle probes as well as using the middle and lower probes for the same combinations of source polarity, high and low source voltages and several NaCl concentrations. This reduced local velocity would allow the reactions involving Cl_2 to take place more readily than without filter paper. Hence more Cl_2, HCl and H^+ is produced resulting in an increased

I_{pri}. The increasing velocity will understandably wash away some H^+ ions in midstream, but more H^+ ions are produced when using the filter paper and reach the cathode than without the paper. Therefore, if the magnitude of the observed current is significantly greater for the case of the wrapped electrode than for the unwrapped electrode, then it would appear likely that the mechanism behind the inverse effect requires an electrode surface in addition to the fact that high voltage and high velocity cause Cl_2 to be washed away with increasing solution velocity. It is noted that the high voltages keep the ion clouds close to the electrodes which create a strong $\vec{E}_{pol}$ and therefore an increased inhibiting current which may be thought to undermine this test, however, the inhibiting current is the same for the case with filter paper and for the case without. Therefore the inhibiting current does not play a big role in the testing of the Cl_2 hypothesis.

The results of the filter paper wrapping tests were negative. The hypothesis appeared to have been refuted. Even though the current was larger if one electrode was wrapped, the effect was essentially the same whether the wrapped electrode was the anode or the cathode (Fig.32). The cathodic reaction, Na^+ to NaOH, occurs spontaneously and consequently does not depend upon the platinum surface.

```
6.0 ──┼──        ──────── +100 v.d.c. without paper                velocity
6.1 ──┼──      ──────────  -100 v.d.c. without paper

7.1 ──┼──       ─────── +100 v.d.c. with paper
7.2 ──┼──      ──────── -100 v.d.c. with paper
```

$|I_{observed}|$ (mA)
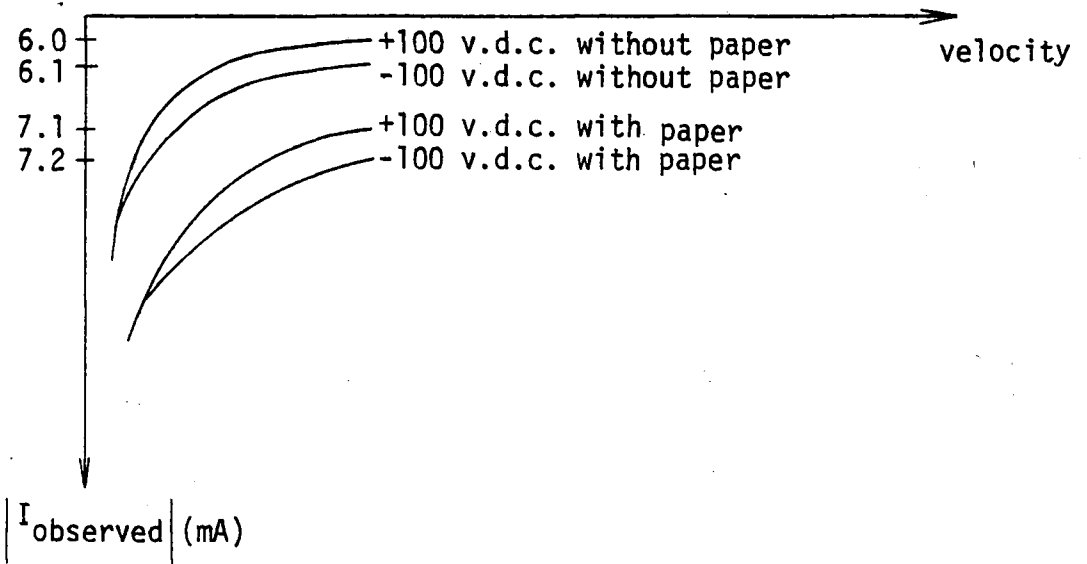
Fig. 32 - Qualitative results of filter paper
           wrapping test

APPENDIX A1

Laminar Flow Calculation

For the experiments that we performed, the flow in the channel was known to be laminar over a portion of the velocity range. Reynolds number for flow between parallel plates (i.e., width of channel assumed[1] to be much greater than depth of channel) is defined as

$$Re = \frac{\rho V h}{\mu}$$

where ρ is the density of the fluid, V is the average free stream velocity, h is the depth of the channel and μ is the dynamic viscosity of the fluid. For this configuration, laminar flow always exists for values of Re less than 1500 [13] but is non-existent for Reynolds numbers greater than 7700. Since the NaCl solutions used were very dilute, the parameters [14] of Reynolds number for plain water may be used and are given in Table V for both of the temperatures that we used.

TABLE V

Parameters For Reynolds Number Calculation
Water

$\rho = 1$ gm/cc $= 1000 Kg/m^3$ $\rho = 1$ gm/cc $= 1000$ Kg/m^3

$\mu = 0.914 \times 10^{-2}$ gm/cm-sec $\mu = 0.610 \times 10^{-2}$ gm/cm-sec

$\mu/\rho = 0.917 \times 10^{-2}$ cm^2/sec $\mu/\rho = 0.616 \times 10^{-2}$ cm^2/sec

The average channel velocity ranged from 0.0 to 48.1 cm/sec (see

---

[1] Assumption is valid since with = W = 8.35 cm and depth = h = 0.59 cm.

-84-

Appendix A2) and the depth of the channel was 0.59 cm. Corresponding to the maximum average channel velocity, the maximum Reynolds numbers for both temperature ranges are:

$$T = 24°C \; : \; Re_{max} = \frac{V_{max}h}{\mu/\rho} = \frac{(48.1 \; cm/sec)(0.59 \; cm)}{0.917 \times 10^{-2} \; cm^2/sec} = 3095$$

$$T = 44°C \; : \; Re_{max} = \frac{V_{max}h}{\mu/\rho} = \frac{(48.1 \; cm/sec)(0.59 \; cm)}{0.616 \times 10^{-2} \; cm^2/sec} = 4607$$

The maximum average channel velocities that yield laminar flows are computed by solving the Reynolds number equation for V and using 1500 for the value of Re:

$$T = 24°C \; : \; max. \; ave. \; velocity = max \; V = \frac{(Re)(\mu/\rho)}{h}$$

$$= \frac{(1500)(0.917 \times 10^{-2} \; cm^2/sec)}{0.59 \; cm}$$

$$= 23.3 \; cm/sec$$

$$T = 44°C \; : \; max. \; ave. \; velocity = max \; V = \frac{(Re)(\mu/\rho)}{h}$$

$$= \frac{(1500)(0.616 \times 10^{-2} \; cm^2/sec)}{0.59 \; cm}$$

$$= 15.7 \; cm/sec$$

These values correspond to actual velocities at the probes, for laminar flow, of 31.3 cm/sec and 20.9 cm/sec (interpolating twice using the first and third tables of Appendix A2) for 24°C and 44°C respectively. Therefore, with absolute certainty, the flow in the channel is laminar for velocities, at the probes, of 31.3 cm/sec or less for 24°C and 20.9 cm/sec or less for 44°C and for average

channel velocities of 23.3 cm/sec or less for 24°C and 15.7 cm/sec or less for 44°C. For velocities greater than those above, flow in the channel could very well be laminar but this is not known with complete certainty.

APPENDIX A2

Rotameter Calibration And Calculation

Of Channel Velocity At Probes

The rotameter (flow meter, F.M.) was calibrated by recording the time required to fill a container with a given volume of water for several rotameter readings. The flow rate in the system was the ratio of the volume of water to the time recorded. The average channel velocity was experimentally computed as the ratio of flow rate (cm^3/sec) to cross-sectional area of the channel (4.92 cm^2) as is shown in Table VI for several flowmeter readings.

TABLE VI

Average Channel Velocities - Experimentally Determined

Flowmeter Reading	Volume of Water per 30 Seconds (Litres)	Flowrate, Vol/time (cc/sec)	Average Channel Velocity (cm/sec)
-6.0[1]	0.000	0.0	0.0
0.0	0.135	4.5	0.9
5.5	0.335	11.2	2.3
10.0	0.700	23.3	4.7
15.0	0.962	32.1	6.5
20.5	1.390	46.3	9.4
25.5	1.770	59.0	12.0
30.5	2.140	71.3	14.5
35.0	2.665	88.8	18.1
39.5	3.115	103.8	21.1
44.5	3.370	112.3	22.8
50.0	3.910	130.3	26.5
55.0	4.610	153.7	31.2
60.0	5.120	170.7	34.7
64.5	5.220	174.0	35.4
70.0	5.830	194.3	39.3
78.0	6.525	217.5	44.0
83.5	7.155	238.5	48.1

[1]Flowmeter readings started at -6.0 since the rest-position of the flow inside the flowmeter was below the zero mark.

The velocity of the electrolyte at the position of the probes was calculated in the following manner: First, the experimentally determined values of the average channel velocity, for each rotameter reading, was compared with the expression for the analytical average velocity in the channel. This comparison allowed computation of the two papameters, a and b, in the equation for the parabolic velocity profile ($v(x) = a - bx^2$) across the channel; again for each F.M. reading. And second, an interpolation was performed to obtain values of the actual velocity at the probes for rotameter readings between those that were taken as data. A spline interpolation was used which operates on four successive data points at a time. A cubic equation is computed through these four points, the portion of the equation through the middle two points is retained as the interpolated data and then the next data point is considered.

The velocity profile in the channel is parabolic as shown in Fig. 33 and is of the form:

$$v(x) = b - ax^2 ,$$

where x is measured from the center of the channel and $v(x)$ is directed downstream. The width of the channel is denoted by 2δ and is equal to 0.59 cm. The boundary conditions are

$$v(\delta) = 0 \text{ and } v(-\delta) = 0$$

which result in

$$a\delta^2 = b.$$

In order to find "a" and "b" we must: (1) compute the analytic average

(a)

Position of probes: x = 0.095 cm
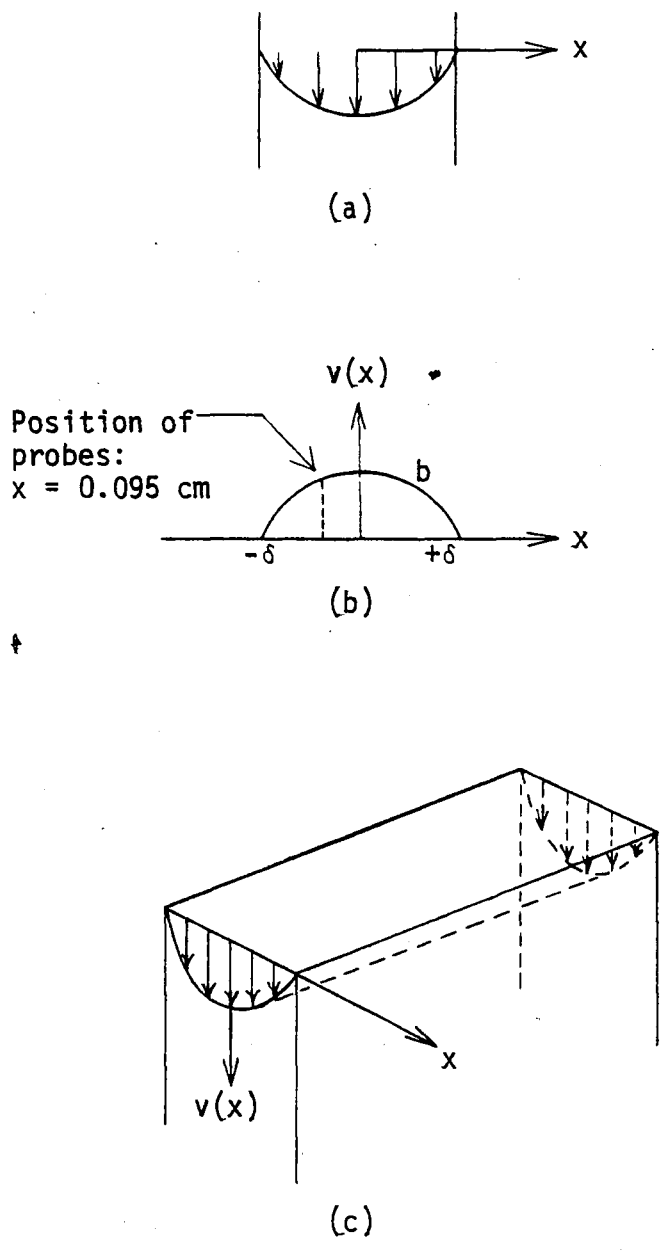
v(x)

b

−δ   +δ

x

(b)

v(x)

x

(c)

Fig. 33 - Velocity profile in channel: (a) side view, (b) analytical representation and showing position of probes, and (c) cut away view

velocity in the channel and set it equal to the experimental average velocity, and (2) use $a\delta^2 = b$ to solve for "b" and then "a" for each flowmeter reading.

(1) The analytic average velocity, $\overline{v(x)}$, is

$$\overline{v(x)} = \frac{\int_{-\delta}^{+\delta} v(x)dx}{2} \equiv \frac{\text{Area under } v(x) \text{ curve}}{\text{Internal}} .$$

The area under the parabolic velocity curve is

$$\text{Area} = \int_{-\delta}^{+\delta} v(x)dx = \int_{-\delta}^{+\delta} (b-ax^2)dx = 2b\delta - \frac{2}{3} d\delta^3 .$$

The analytic average velocity is therefore

$$\overline{v(x)} = \frac{2b\delta - \frac{2}{3} a\delta^3}{2\delta} = b \frac{a\delta^2}{3} = \overline{v}$$

and using $a\delta^2 = b$ results in

$$\overline{v} = \frac{2}{3} b.$$

(2) The following Table contains the experimental average velocity and the values of "a" and "b" for each flowmeter reading.

TABLE VII

Calculation Of Velocity Profile For Each F.M. Reading

F.M. Reading	Experimental Average Velocity $\bar{v}$ (cm/sec)	$b = \frac{3}{2}\bar{v}$ (cm/sec)	$a = \frac{b}{\delta^2}$ (cm/sec)$^{-1}$
-6.0	0.0	0.0	0.0
0.0	0.9	1.4	15.7
5.5	2.3	3.4	39.3
10.0	4.7	7.1	81.7
15.0	6.5	9.8	112.4
20.5	9.4	14.1	162.2
25.5	12.0	18.0	206.7
30.5	14.5	21.7	249.8
35.5	18.1	27.1	311:1
39.5	21.1	31.7	363.7
44.5	22.8	34.3	393.5
50.0	26.5	39.7	456.4
55.0	31.2	46.9	538.5
60.0	34.7	52.1	598.1
64.5	35.4	53.1	609.7
70.0	39.3	59.0	678.1
78.0	44.0	66.0	758.4
83.5	48.1	72.1	828.4

The position of the probes in the channel was at $|x| = 0.095$ cm and hence the absolute velocity at the probes, for each flowmeter reading that was taken, is calculated from $v(-0.095) = a-b(0.095)^2$ where "a" and "b" are known. The results are shown in Table VIII

TABLE VIII

Velocity At Probes Vs. Flowmeter Reading

Flowmeter Readings	Absolute Velocity At Probes (cm/sec)
-6.0	0.0
0.0	1.2
5.5	3.1
10.0	6.4
15.0	8.8
20.5	12.7
25.5	16.1
30.5	19.5
35.5	24.3
39.5	28.4
44.5	30.7
50.0	35.6
55.0	42.0
60.0	46.7
64.5	47.6
70.0	52.9
78.0	59.2
83.5	64.6

Interpolating between the above values yields the following graph of channel velocities at the probes versus flowmeter readings.
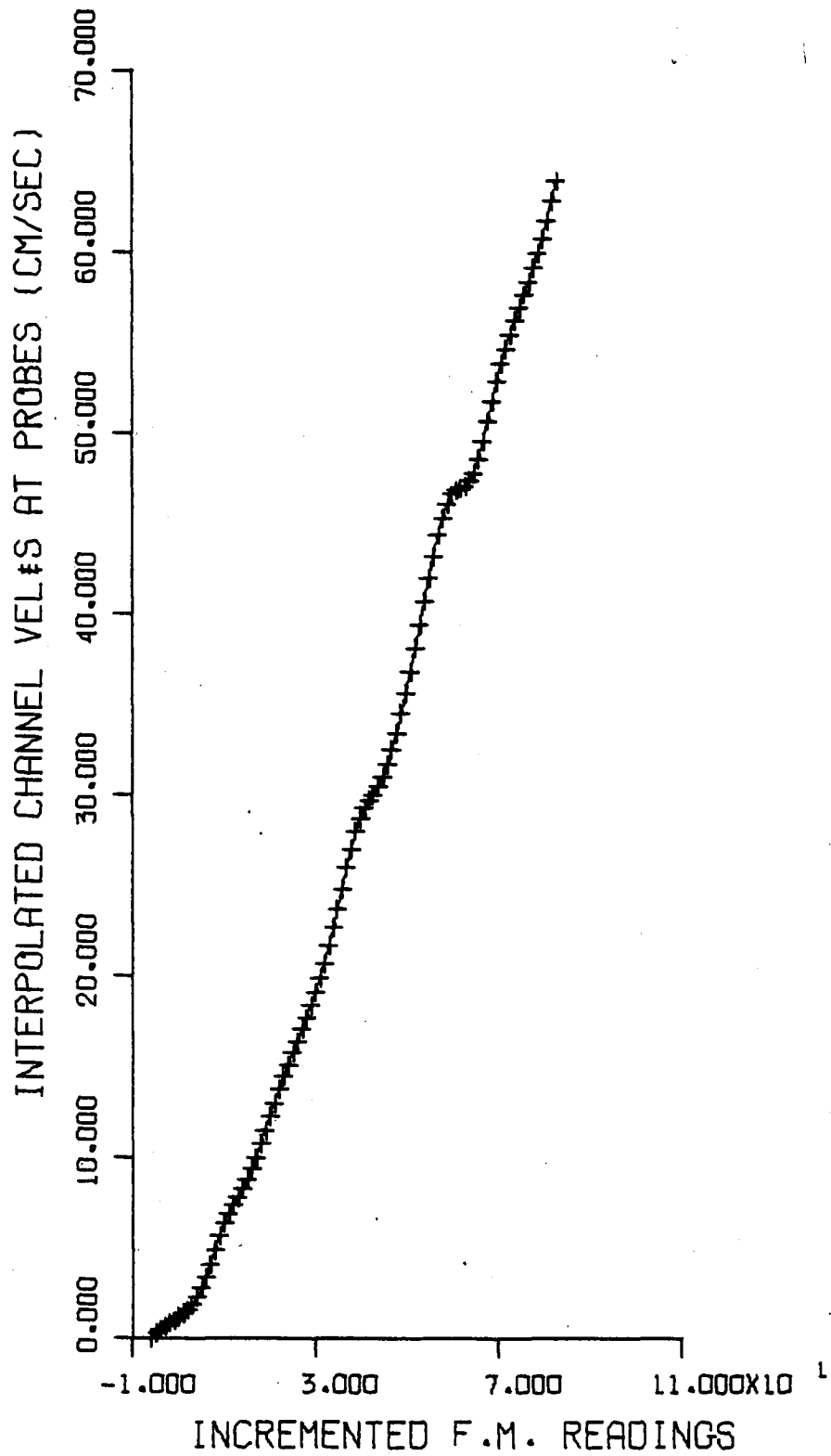
Fig. 34 - Flowmeter calibration

APPENDIX A3

On The Dilution Of The Electrolyte Used

The following addresses the question of to what degree of infinite dilution were the sodium chloride solutions that we used. The high (soln #3) and low (soln #4) concentrations were 2.052×10^{-3} and 4.104×10^{-4} molar NaCl respectively. Since these electrolytic solutions were of type 1-1, their concentrations expressed in moles of solute per liter and number of equivalents per liter are equal. The graph of molar conductances versus square roots of concentration, shown on the following page [15] is therefore applicable, and in particular, the insert showing the curve for KCl, also a type 1-1 electrolyte, is of interest. Taking the square root of the concentrations that were used yields approximately 0.045 and 0.020 equivalents per liter. The insert therefore shows that the concentrations were approximately 96 and 98 percent infinitely dilute. In other words, regarding conductivity discussions, the solutions that we used were less than 5 percent from being infinitely dilute. Hence the chapter of electrolytic conductance theory is applicable to the solutions that were used.
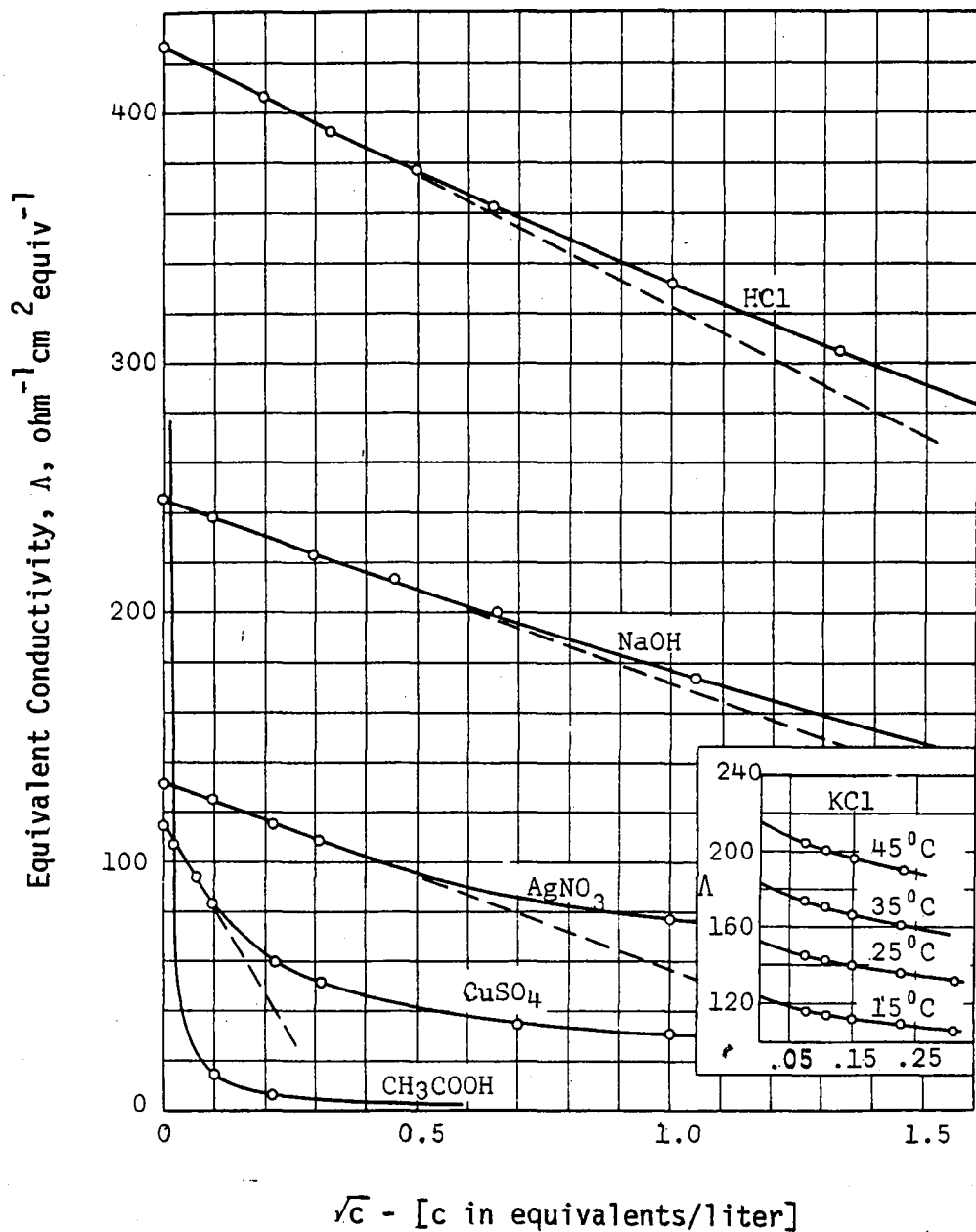
Fig. 35 - Molar conductances at 298.15 K of electrolytes in
aqueous solution vs. square roots of concentrations.
Insert shows variation with temperature of Λ for
KCl

Timing Circuit For Pulsing Electrodes

In addition to applying a voltage pulse of known amplitude and duration to the pair of probes, it was desired to trigger the oscilloscope some given time before the pulse started and before it ended. These two triggering times allowed detailed observation of the probe current just before and during the application of the voltage pulse ("on"state) as well as just before and after the removal of the pulse ("off" state). A reed relay was used to open and close a circuit (in which the source voltage was in series) and hence remove and apply the voltage respectively. Fig. 36 shows a timing diagram for the application of the pulse as well as the two triggering times, trg(a) and trg(b).

A simple but adequately accurate circuit was designed and built to implement this diagram and is shown in Fig. 37 while its pertinent waveforms are shown in Fig. 38 . The circuit consist of timers which output pulses of variable duration which are used for the triggering requirements as well as for the inputs to an OR gate. Essentially, one input causes the relay to close and the other input causes it to open. The OR gate is connected to a toggling J-K flip-flop whose output drives a transistor switch, which in turn drives the relay.

More specifically, the first timer was configured as a free running oscillator whose pulse width was approximately 0.65 ms and
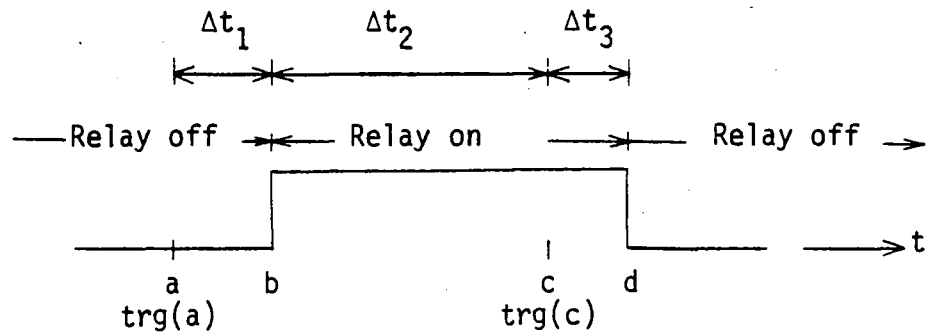
Fig. 36 - Timing diagram for application of voltage pulse
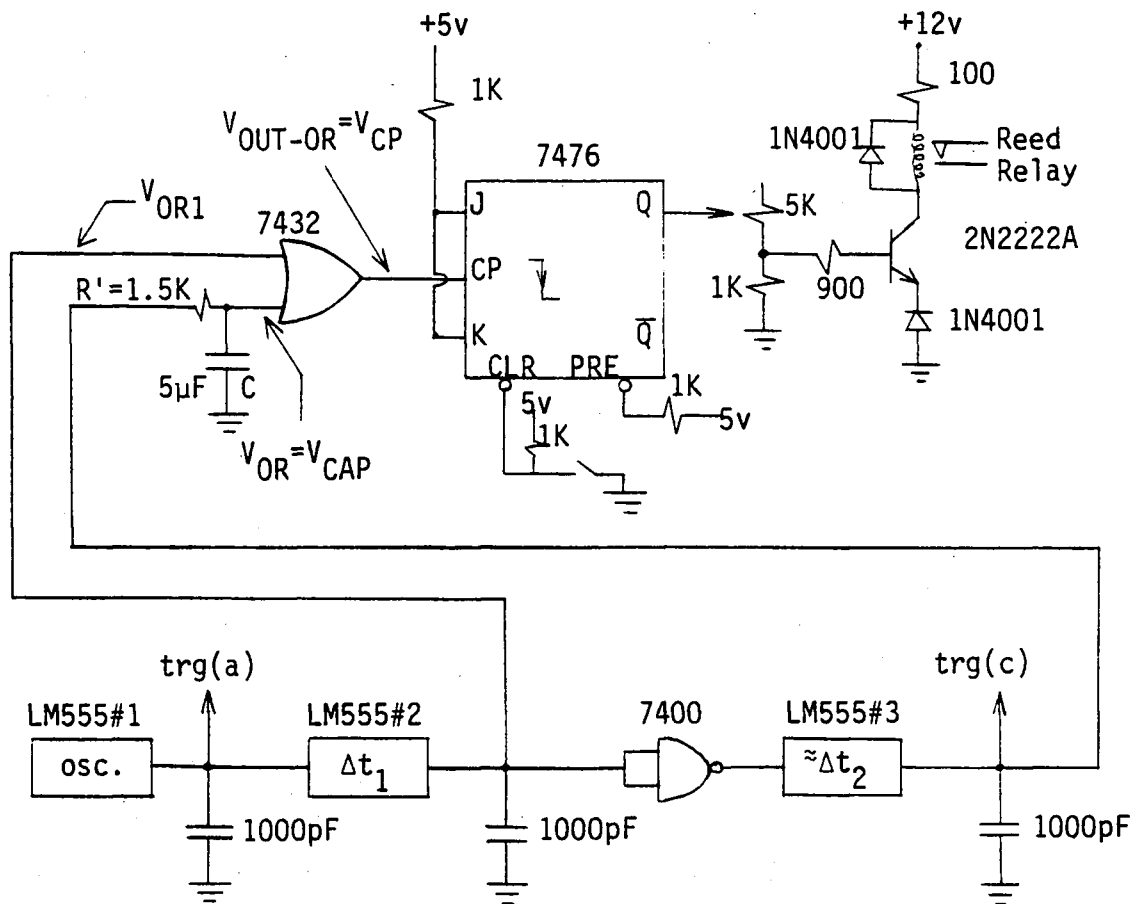

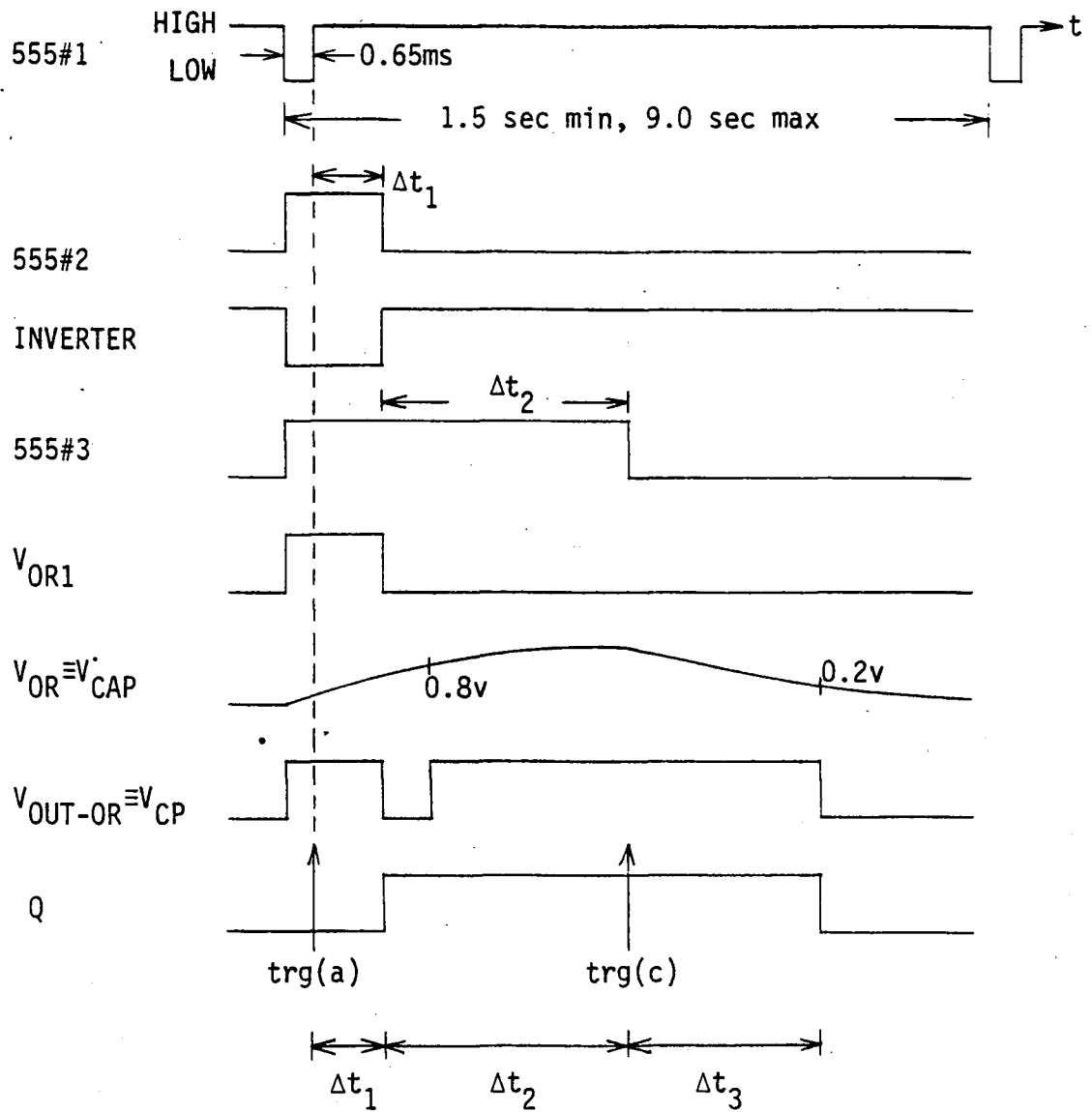Fig. 37 - Circuit for automatic application of voltage pulse

Fig. 38 - Schematic representation of pertinent waveforms of timing circuit (neglecting gate delays and absolute amplitudes)

whose frequency was variable between 1.5 and 9.0 seconds. This timer facilitated repeated pulse applications automatically. The falling edge of timer number one's output caused the second and third timers to output pulses of predetermined durations. The pulse width of timer #2 minus that of timer #1 yielded the duration of time between trg(a) and the application of the voltage pulse - since the rising edge of timer number one's output caused trg(a) to occur. The pulse width of timer #2 also caused the output of the OR gate to go "high" for the same amount of time. The Precleared flip-flop, which is negatively edged triggered, then put out a high value when timer #2 went low, i.e., the inverter went high. The transistor and relay were turned on and the source voltage, V_1, was applied. The pulse width of timer #3 is approximately equal to the "on" time of the relay. This statement becomes more accurate as Δt_1 and Δt_3 are decreased as seen in Fig. 38. After the OR gate went high when it received a pulse on its upper input, its output would again go high when the voltage at its lower input exceeded 0.8 volts. This would occur after timer #3 put out its pulse and at a time determined by R' and C - this time is called t_{charge}, or t_{ch} and the associated time constant is $\tau_{ch} \approx (R'||4K)C$. The output of the OR gate would remain high until a given time after the pulse from timer #3 was removed, this time was called $t_{discharge}$, or t_{disch} and was again determined by R' and C with $\tau_{disch} = R'C$. After the duration of t_{disch}, the voltage across capacitor C would fall below 0.2 volts at which time

the output of the OR gate would go "low", thus toggling the flip-flop into a low output state, turning both the transistor and relay off resulting in the removal of the voltage pulse from the probes. The falling edge of timer #3's output was used as the signal for trg(c). It is noted that t_{ch} must be greater than Δt_1 in order to allow the output of the OR gate to go low which initially triggered the flip-flop and hence applied the source voltage to the probes; if Δt_0 was greater than t_{ch}, the OR gate would not go low until timer #3's output went low thereby destroying the desired timing sequences. It was desirable to obtain minimum values of Δt_0 and Δt_3; however, the previous requirement on t_{ch} and Δt_1 put a lower limit on these minimum values. If, for example, t_{ch} was to be increased by increasing R'C, then t_{disch} would also increase and so would Δt_3 since t_{disch} was identical to Δt_3 (see Fig. 38). Another example is a decrease in Δt_3, or t_{disch}, in order to examine the probe current close to the occurrence of the on-to-off transition of the applied voltage. Decreasing t_{disch} is accomplished by reducing R' which also decreases t_{ch}, but t_{ch} must always be greater than Δt_1, the latter determining the placement of trg(a) and whose value is usually selected before the other parameters. The 1000pF capacitors placed on the output of the timers eliminated false triggering of successive devices.

REFERENCES

[1] Fuoss, Raymond M. and Accascina, Filippo, _Electrolytic Conductance_, Interscience Publishers, Inc., New York, 1959, Ch. 1.

[2] Prutton, Carl F. and Maron, Samuel H. _Fundamental Principles of Physical Chemistry_, The Macmillan Company, New York, 1956, p.459.

[3] Ibid., p.215.

[4] Ibid., p.221.

[5] Ibid., p.223.

[6] Potter, Edmond C. _Electrochemistry, Principles and Applications_, The Macmillan Company, New York, 1956, p.145.

[7] Ibid., p. 148.

[8] Ibid., p. 131.

[9] Ibid., p. 132.

[10] Hartill, E. R., McQueen, J. G., and Robson, P.N. "A Deep Electrolytic Tank for the Solution of 2- and 3-Dimensional Field Problems in Engineering," Institution of Electrical Engineers, Paper no. 2179 M, Oct. 1956.

[11] Bockris, J. O'M. and Drazic, D.M. _Electro-Chemical Science_, Barnes & Noble Books, New York, 1972, pp.118-125.

[12] Prutton, Carl F. and Maron, Samuel H. _Fundamental Principles of Physical Chemistry_, The Macmillan Company, New York, 1956, p.459.

[13] Potter, Merle C. and Foss, John F. _Fluid Mechanics_, John Wiley and Sons, Inc., New York, 1975, p.282.

[14] Baumeister, Theodore, Avallone, Eugene A., and Baumeister III, Theodore. _Mark's Standard Handbook for Mechanical Engineers_, 8th ed., McGraw-Hill, Inc., New York, 1978.

[15] Moore, Walter J. _Physical Chemistry_, Prentice-Hall, Inc., Englewood Cliffs, New Jersey, 1972, p.426.

VITA

Wayne Stephen Groh was born in Mineola, New York on May 4 1956 to Coral R. and Joel B. Groh. He graduated from Ramsey High School, Ramsey, New Jersey in 1974. Mr. Groh attended Lehigh University in September 1974 where he graduated with honors and received the degree of Bachelor of Science in Electrical Engineering in May 1978. Since then, he has been a teaching assistant in Electrical Engineering at Lehigh University.